

1615 Type I Interferon Signaling Mediates Toxic Shock-Like Syndrome Induced by Intracellular Bacteria

HL Stevenson, Q Yang, M Scott, N Ismail. UPMC, Pittsburgh, PA.

Background: *Ehrlichia chaffeensis* is an obligately intracellular bacterium that causes fatality by inducing toxic shock-like syndrome and provides an excellent model of immune-mediated liver pathology. The liver is the primary site of pathology and infection results in extensive hepatocyte necrosis and apoptosis, which is associated with over activation of the immune response including secretion of inflammasome-dependent IL-1 β and IL-18, and expression of IFN α/β . Although selectively inhibiting the main pathogenic immune cells such as neutrophils, NK, and CD8⁺ T cells is partially protective resulting in prolonged survival and decreased pathology, the key event that leads to over activation of immunity is not known.

Design: Although type I interferons are well known for providing critical defense against viruses and bacteria, they have recently been shown to promote sepsis. We hypothesized that activation of the inflammasome pathway by NLRP3, caspase 1, and/or type I IFN may be the key event leading to immunopathology in our model of toxic shock-like syndrome. We addressed the role of type I interferons by examining *Ehrlichia* infection of C57BL/6 mice lacking type I IFN receptors (IFN α/β R^{-/-}).

Results: Surprisingly, infected IFN α/β R^{-/-} mice were completely protected against a normally lethal dose of bacteria and survived past 30 days post-infection. Protection of the IFN α/β R^{-/-} mice correlated with effective bacterial clearance, altered pathology, increased IFN- γ in sera, decreased IL-10 in sera and spleens, and increased frequency of protective CD4⁺ Th1 and NKT cells in the spleen. Furthermore, lack of IFN α/β R signaling significantly abrogated production of IL-1 β , suggesting that inflammasome activation during lethal disease is linked to IFN α/β signaling. To test this possibility, we infected NLRP3^{-/-} and Caspase 1^{-/-} mice with *Ehrlichia*. Compared to complete protection of IFN α/β R^{-/-} mice, NLRP3^{-/-} and Caspase 1^{-/-} mice were only partially protected. These mice also had lower bacterial burdens, attenuated hepatic necrosis and apoptosis, and decreased expansion of neutrophils. Interestingly, production of type I IFN was lower in NLRP3^{-/-} and Caspase 1^{-/-} mice than in WT mice, but was not completely abrogated. The latter could account for incomplete protection of these mice, and suggests that type I IFN signaling plays a major pathogenic role upstream of the NLRP3 inflammasome.

Conclusions: IFN α/β signaling is a master regulator of fatal intracellular bacteria-mediated toxic shock-like syndrome and warrants further investigation in human sepsis-like syndromes.

Informatics

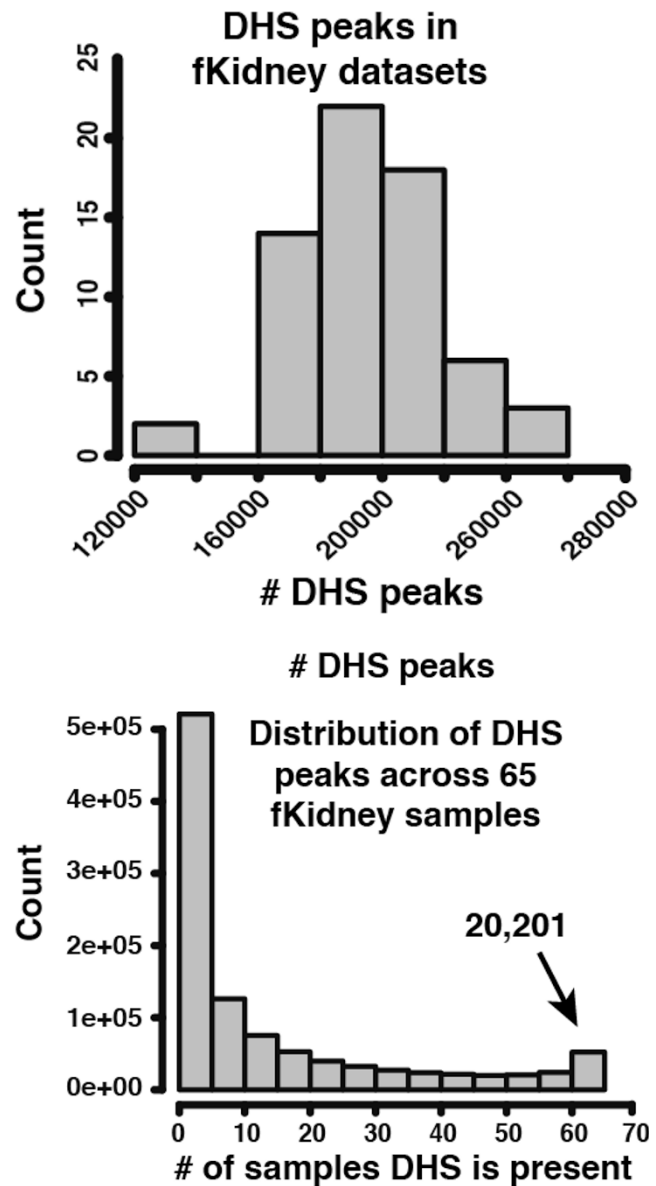
1616 Regulatory Genomics of the Kidney Illuminated by DNaseI-seq

S Akilesh, JA Stamatoyannopoulos. University of Washington, Seattle, WA.

Background: A fundamental role for epigenomic defects and altered transcriptional regulatory programs in the pathogenesis and clinical biology of both neoplastic and non-neoplastic disease is increasingly evident. However, we still lack basic knowledge of the functional genomic architecture of major tissues, creating a major obstacle to systems-level approaches for understanding and treating disease. New technologies now allow us to surmount this bottleneck to efficiently map regulatory DNA (e.g. promoters, enhancers, insulators) on a genomic scale.

Design: Regulatory DNA is characterized by the cooperative binding of sequence-specific transcriptional regulatory factors in place of a canonical nucleosome, leading to an altered chromatin state that is characterized by markedly heightened accessibility to nucleases such as DNaseI. DNaseI treatment followed by high throughput sequencing was previously applied to kidney tissue (n=65 from day 82-147 fetuses) and the resulting datasets were deposited in the NIH Roadmap Epigenomics Mapping Consortium (NREMC) database. We are applying novel bioinformatic analyses developed for the ENCODE project (~30 papers *Nature, Cell, Science*, 2012) to understand the changing regulatory landscape of the kidney during development.

Results: Preliminary analysis of fetal kidney datasets reveals a wide range of DNaseI hypersensitive sites (DHS) in fetal kidney tissues (range 128,051-247,500, Fig. 1).



While many DHS are present only in a few samples, a set of 20,201 DHS are present in all fetal kidney tissues analyzed (Fig. 2). Further evaluation of these conserved and differentially expressed DHS is in progress to mine the regulatory DNA landscape of the kidney.

Conclusions: Global DHS profiling using DNaseI treatment and next-generation sequencing technologies will provide novel insights into the changing regulatory DNA landscape of the kidney.

1617 Synoptic Report Generators for Hematopathology: Development of a System Embedded within the Anatomic Pathology Laboratory Information System (APLIS) That Integrates Morphology, Flow Cytometry, Immunohistochemistry and Molecular Genetics

A Alkhasawneh, JR Ross, CM Carter, SZ Al-Quran, Y Li, RW Allan. University of Florida, Gainesville, FL.

Background: Synoptic reporting for cancer specimens have increased the consistency, completeness of reporting, ease of interpretation and creating of discrete value reporting that allows for ease in data mining. APLIS systems now contain embedded synoptic reporters for cancer cases, but such systems do not handle the complex reporting of hematopathology specimens and do not allow for synoptic reporting of morphology, flow cytometric, immunohistochemical and molecular genetic findings. We sought to develop an embedded custom synoptic report generator for transplantation pathology specimens using our anatomic pathology laboratory information system (APLIS) (PowerPath, SunQuest).

Design: We developed custom synoptic reporting- based embedded templates using the worksheet function within our APLIS (PowerPath) for hematopathology specimens. The programming is easy to perform and using standard choice fields: drag and drop, multiple choice, complex choice and free text reporting options. These synoptic checklists included pertinent morphologic findings (degree of dysplasia, qualitative assesment of lineage maturation, blast counts), flow cytometric findings (antibody and corresponding intensity), immunohistochemistry (antibody performed, qualitative and quantitative result for certain antibodies such as CD34, CD138). In addition, karyotype

and FISH findings were also included with common abnormalities available as check box selects. Pertinent molecular genetic findings were also included (FLT3 mutation, NPM mutation, CEBPA mutation- for example).

Results: The embedded synoptic worksheet reports had the following advantages of standard reporting: 1) improved ease of reporting; 2) standardization of reporting; 3) ability to generate searchable results that include the correlation of all parameters of a given case (morphology, flow cytometry, immunohistochemistry, molecular genetics); 4) potential to integrate into the health system wide integrated data repository (IDR) which can allow for correlation/ biomarker discovery and allow for an easy interface to the health system biorepository.

Conclusions: Embedded synoptic report generators for hematopathology within an APLIS improves consistency, completeness, accuracy, and better integration of results for additional benefits for future research.

1618 Synoptic Report Generators for Transplantation Pathology: Development of a System Embedded within the Anatomic Pathology Laboratory Information System (APLIS)

RW Allan, LV Duckworth, LR Dixon, DS Rush, CM Carter. University Florida, Gainesville, FL.

Background: Synoptic reporting for cancer has increased the consistency, completeness of reporting, ease of interpretation and creating of discrete value reporting that allows for ease in data mining. Most modern APLIS have some embedded capability to generate cancer site specific synoptic reports. There are no reports of similar synoptic report generators that address the standard reporting elements for pathology transplantation follow-up specimens. We sought to develop an embedded custom synoptic report generator for transplantation pathology specimens using our anatomic pathology laboratory information system (APLIS) (PowerPath™, SunQuest).

Design: We developed custom synoptic reporting- based embedded templates using the worksheet function within our APLIS (PowerPath™) for the different transplant biopsy specimens (lung, heart, liver). The programming is simple with drag and drop choice, multiple choice, complex choice and free text reporting options. These synoptic checklists included significant reporting elements (grade of rejection, inflammation, infectious agents, presence of recurrent native disease (for example HCV in liver transplant biopsies) and also quality assurance measures such as the adequacy of biopsy (number of pieces of alveolated lung, adequacy of heart biopsies). Discrete value reporting into our hospital electronic health record (EHR) (Epic Systems, Verona, WI) also affords the opportunity to create flagged results to alert clinicians to biopsies with significant findings (rejection, infection). Integration with the hospital system integrated data repository (IDR) is also planned to allow for correlation/ discovery with clinical and laboratory information.

Results: The embedded synoptic worksheet reports had the following advantages of standard reporting: 1) improved ease of reporting; 2) standardization of reporting; 3) ability to create flagged/ significant results in the hospital EHR; 4) development of quality assurance reports addressing the rates of adequacy of biopsies and rates of rejection for individual pathologists; 5) free text fields which allow some flexibility in reporting or addressing particular clinical questions; 6) improved research applications including the ability to search the discrete data values.

Conclusions: Embedded synoptic report generators for transplantation pathology within an APLIS improves consistency, completeness, accuracy, ease of reporting, interpretation with ability to flag abnormal results and allows for easier quality assurance tracking and research applications.

1619 Utility of Non-Medical Voice Recognition Software for Transcription of Pathology Reports

M Amin, S Roy, AV Parwani, B Tandon, L Pantanowitz. Affiliated Pathologists Medical Group, Torrance, CA; UPMC, Pittsburgh, PA.

Background: Voice recognition software (VRS) has been used by pathologists to construct diagnostic reports. Both non-medical and medical versions of VRS exist, of which the medical version theoretically provides greater accuracy when challenging medical terms are used. However, medical versions of this software are typically more expensive, which may limit their availability to smaller laboratories. We compared the medical version of Dragon Naturally Speaking for Mac (MDNS) (Nuance, Burlington, MA, \$999) with two non-medical versions of VRS, Dragon Dictate for Mac (DD) (Nuance, \$199) and Dictation in OS X Mountain Lion (DML) (Apple, Cupertino, CA, free).

Design: Seven pathologists completed basic voice training in both MDNS and DD. Voice training was not a component of DML. Each pathologist dictated the same set of 7 pathology reports composed of various diagnostic lines and comments. Each pathologist used the same wired headsets, computers (MacBook Pro 2012) and high-speed Internet connection for access. Following each dictated report, the number of transcription errors was recorded. Given the ability of both MDNS and DD to customize how words are interpreted, each pathologist was allowed to re-train words of his/her choice following the dictation of each report.

Results: Error rates are shown in table 1. While the fewest errors occurred initially with MDNS, both MDNS and DD performed equally well after additional voice training. DML recognized several pathology terms without requiring any voice training, but misinterpreted terms not found in standard dictionaries. DML also required persistent Internet access, while MDNS and DD did not. Error rates decreased when complete sentences were used with all VRS types. For each VRS, error rates varied among pathologists, possibly due to dictation speed, style and different accents.

Table 1. Transcription Error Rates for Each Voice Recognition Software

Voice Recognition Software	Range of Error Rates (and Average)	Range of Error Rates (and Average), Following Additional Training
MDNS	5-15% (8%)	1-5% (2%)
DD	9-27% (12%)	1-5% (2%)
DML	62-89% (75%)	59-91% (75%)

MDNS: Dragon Naturally Speaking, medical. DD: Dragon Dictate, non-medical. DML: Apple Dictation.

Conclusions: With minimal additional training, non-medical VRS such as DD is feasible for dictation in a pathology practice, with similar performance to MDNS but at a lower cost. With no voice training capability to enhance the recognition of pathologic terms, DML is unreliable for the transcription of pathology reports.

1620 Successful Validation of Virtual Microscopy for Surgical Pathology but Not Cytopathology: Application of the College of American Pathologists (CAP) Guidelines

MA Arnold, EA Chenever, KK Nicol, T Barr. Nationwide Children's Hospital, Columbus, OH.

Background: Virtual microscopy is rapidly emerging as a key technology for transforming educational and diagnostic services. Recently, CAP published the first guidelines for validating the diagnostic virtual microscopy. Herein, we report the findings of virtual microscopy validation for surgical pathology and cytopathology specimens at our pediatric institution.

Design: The study set consisted of a combination of randomly selected cases and cases selected to represent complex or less common diagnostic categories. Surgical pathology specimens served as a primary modality (60 cases with 130 specimen parts) and cytopathology as a secondary modality (21 cases with 33 specimen parts).

Study Cases

Cytopathology	
BAL	7
CSF	6
FNA	4
Bone marrow	4
Surgical Pathology	
CNS resection	12
GI biopsy	10
Heart biopsy	3
Liver	3
Lung biopsy	1
Other	8
Placenta	3
Skin	5
Suction rectal	1
Tonsil	8
Tumor	6

In total, the study included 627 slides. Cases were reviewed by the 9 pathologists who had previously completed clinical evaluation of the glass slides, and in accordance with the CAP guidelines. Digital slides corresponding to those ordered by the pathologist (special stains and immunohistochemical stains) and ancillary test results were available to the pathologist on request after initial digital slide review.

Results: Based on our previous experience, digital capture of cytospin slides and small biopsies was performed at 40x magnification. The remaining slides were captured at 20x magnification in a single plane. Low cellularity prevented capture of 2 cytology slides, precluding evaluation of one case. Of the surgical pathology cases, the final diagnoses were highly concordant with glass slide diagnoses; major diagnostic discrepancies were seen in 1.7% of cases (2.3% of specimen parts), and none altered patient management. Diagnoses for cytology specimens were significantly more discordant, with major discrepancies or inadequate cytologic detail for confident review in 25% of cases (31% of specimen parts).

Conclusions: Our results demonstrate that surgical pathology specimens representing the spectrum of pediatric pathology practice can be adequately reviewed when using virtual microscopy validated with the CAP guidelines. However, review of cytology specimens will require improved resolution, perhaps including image capture of multiple focus planes.

1621 A Pipeline for Curation of Genetic Variants through OMIM

B Baskovich, K Upadhyay, H Ostrer. Montefiore Hospital/Albert Einstein College of Medicine, New York, NY.

Background: Interpreting genetic variants remains a difficulty of high-throughput genetic testing. The Online Mendelian Inheritance in Man (OMIM) website provides a curated database of over 12,000 genes and their variants with interpretations of pathogenicity, explanations and literature sources. Algorithms including SIFT, PolyPhen2, and Mutation Taster consider amino acid change, location in the protein, and conservation. One method of dealing with the uncertainty in pathogenicity is to provide a confidence level; the International Agency for Research on Cancer (IARC) has developed a scoring system on a scale of 1 to 5, from almost certainly nonpathogenic to almost certainly pathogenic (3 being indeterminate).

Design: Axiom microarrays were performed on 196 members of each of the Bronx's 3 majority ethnic groups: African Americans, Puerto Ricans, and Dominicans. Pooled whole-exome sequencing was also done on the Dominicans. A pipeline was written in BioPerl to parse the results and query OMIM and ClinVar based on the variants' nucleotide position. Useful parameters were extracted from these and other databases including pathogenicity, 1000Genomes results and ESP6500 results. For all results called pathogenic, literature sources were manually reviewed and an IARC score was assigned. Scores were also obtained from SIFT, Polyphen2, and MutationTaster.

Results: The Axiom software called 305,513 variants. The pipeline resulted in 1440 known variants of which 338 were reported as pathogenic. Of the more common

variants, the majority were given an IARC score of 3 (35%) or 4 (42%). However, 10% were considered likely nonpathogenic (1 or 2) after reviewing the literature. Several variants had allele frequencies too high to be pathogenic given the disease prevalence. Whole-exome sequencing identified 62 additional pathogenic variants per OMIM in the Dominicans, 19 of which we scored a 4 or 5. There was no correlation in IARC scoring results with the algorithms' results. The results among the three programs also varied widely (55% of the variants had one prediction opposite the others).

Conclusions: A large number of variants identified as pathogenic by OMIM and ClinVar were determined to be inconclusive or polymorphic upon review. Most of those called 1 or 2 were actually identified as polymorphic by the papers cited in OMIM. Most calls of 3 were made due to weak evidence such as one patient who was a compound heterozygote. The variation with the scoring algorithms is not surprising, as our scoring was based on the literature (linkage studies and functional studies), whereas the algorithms consider the amino acid change.

1622 Development of CaTissue Suite as a State-of-the-Art Integrated IT Management System for Solid and Liquid Research Biospecimens and Their Molecular Derivatives

D Chadwick, H Begley, G Disney, N Qazi, A Alam, A Ali, N Amin, M Cardoso, J Cheung, M Chasmar, T Dookhie, J Jiang, R Kwok, S-B Liang, F Meng, S Shaw, I Slavine, V Son, M Sukhram, T Michaelson, MHA Roehrl. University Health Network, Toronto, ON, Canada.

Background: caTissue Suite is an open-source web-based research biospecimen management system developed by the NCI and highly customized and integrated into the overall BioSpecimen Sciences IT infrastructure of one of North America's largest research biobanking programs.

Design: Requirements for customization of the system included: tracking, collection, storage, and distribution of all biospecimens and molecular derivatives (DNA, RNA, protein, metabolites, etc.), labeling biospecimens with numeric and 2-D barcodes, interfacing with the Electronic Patient Record (EPR) and CoPath, creating custom queries, documenting basic clinical and study information including consent, and federating caTissue Suite with other research databases, such as cancer genomics and other multidimensional data-rich molecular repositories.

Results: Complex banking and distribution of all biospecimens have been accomplished in caTissue Suite. Biospecimens include solid tissues from surgical resections, biopsies and autopsies (fresh, snap frozen, FFPE, tissue sections, DNA), blood (whole blood, serum, plasma, buffy coat, DNA) and body fluids (fresh, frozen cell pellets and supernatant, cytospin slides). More than 10 years (over 200,000 biospecimens) of legacy data are being imported. Scanner and human-readable numeric and 2-D barcode labels are printed onto cassettes and vial labels. Demographic information is imported through an interface with EPR, and an HL7 feed dynamically imports pathology reports from CoPath. Custom queries have been created to search for upcoming procedures (surgery, autopsy, venipuncture, paracentesis) and verify consent status. Basic clinical data (tentative disease status, preoperative treatment, frozen section diagnosis) and research study/trial information are also documented. caTissue Suite has been federated with Caisis (clinical annotation database) via SAP technology, to facilitate sophisticated custom searches combining biospecimen, clinical, and research data.

Conclusions: caTissue Suite has been implemented as a very powerful state-of-the-art research biospecimen management system for documenting, tracking, and annotating a large and diverse collection of biospecimens and derivatives for use in basic, translational, and clinical trial research studies. A federated BioSpecimen IT infrastructure has been created linking clinical and research domains.

1623 Digital Hematopathology for Tumor Board Increases Efficiency and Clinical Team Satisfaction

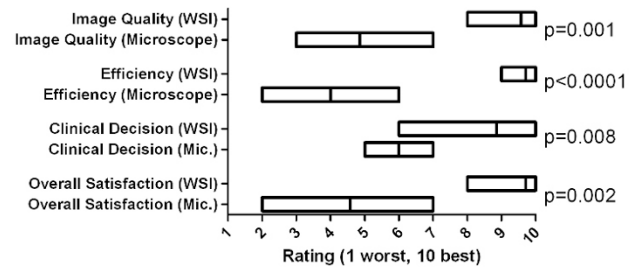
ZW Chen, J Kohan, B Sweeten, JW Hussong, SL Perkins, ME Salama. University of Utah/ARUP Labs, Salt Lake City, UT.

Background: Whole slide imaging (WSI) is widely used for education and research but is increasingly being used to streamline clinical workflow. We present our experience with regards to satisfaction and time utilization, including using oil immersion WSI for blood/marrow aspirate smears in hematology tumor board (TB)/clinical care conferences, allowing for excellent morphologic detail.

Design: Using Aperio XT & CS-O slide scanners, lymph nodes and core biopsies were scanned at 20X magnification and blood/marrow smears at 100X under oil immersion and uploaded to an online library (Aperio eSlide Manager) with areas of interest annotated digitally to be displayed via a standard web browser. Time required to identify scanning areas and annotate was compared to microscope projection (MP), which required moving to cells of interest on each slide on a microscope connected to a video camera/projector. A 10-point evaluation survey was used to assess clinical staff satisfaction with each presentation method.

Results: There was no significant difference in slide selection, annotation and eSlide display time compared to total time with MP. However, a different time distribution allowed for increased efficiency during TB as selection and annotation of slides was done prior to TB with WSI rather than during TB with MP. Technician time for oil immersion slide scanning averaged 9.7 min/slide (range 5-23 min depending on scan area). Survey results (78% response rate) showed a significant increase in satisfaction by clinical attendees with regard to image quality, efficiency of presentation of pertinent findings, aid in clinical decision-making and overall satisfaction regarding pathology presentation (mean of differences 2.9-5.7 for each criteria; all $p < 0.01$ t-test).

Results of Satisfaction Survey



A majority of respondents also noted decreased motion sickness with WSI.

Conclusions: WSI provides higher quality images compared to MP and significantly increases clinician satisfaction. WSI streamlines preparation for TB by permitting prior slide and cell selection, resulting in greater efficiency during TB presentation. Despite increased preparation time needed for oil slide scanning, WSI shifts time requirements to technicians and increases efficiency for pathologists and clinicians, resulting in an improved overall TB experience.

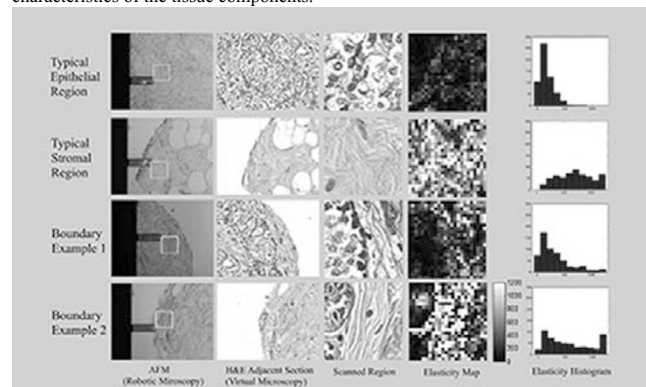
1624 Atomic Force Microscopy Visualizes Different Tissue Elasticity: A Novel Diagnostic Tool for Pathologist

W Chen, H Zhong, R Roy, J Desai, L Goodell, D Foran. Rutgers Robert Wood Johnson Medical School, New Brunswick, NJ; University of Maryland, College Park, MD.

Background: Different cellular components differ in their mechanical properties, for example, tissue elasticity. Atomic force microscopy (AFM) is a novel tool that can probe tissue elasticity, which has been used in studying cultured cells, fresh tissue and microorganisms, but not on formalin fixed and paraffin embedded (FFPE) tissue sections. This initial study was designed to investigate the feasibility of combining digital pathology with AFM for potential clinical application through characterizing tissue elasticity on histopathology tissue sections.

Design: Tissue microarrays were constructed from a set of archived FFPE breast specimen. One 4- μ m section was sampled and deparaffinized for AFM scan. An adjacent H&E section was digitized on a whole slide scanner. Targets of each sample for AFM were annotated by pathologists, which was blinded to the study using a standard web interface for viewing. Digital pathology techniques were incorporated to facilitate image and data processing.

Results: Based on the study design, different histological components of breast tissue were sampled by AFM, including benign and malignant epithelium, various stromal components, as well as epithelial/stromal boundary regions. During the course of these experiments, the prototype setup allowed quick, reliable visualization of the differences in elasticity signature across the constituent tissue components as a function of the spatial distribution. Examples were shown in figure 1. Typically, epithelial region showed distinctively low elasticity modulus readings compared to fibrous stroma. The boundary region displayed precise localization of and clear distinction between elasticity characteristics of the tissue components.



Conclusions: This preliminary study demonstrates that AFM is capable of distinguishing different tissue components based on elasticity, suggesting potential clinical utility. In addition, our team plans to utilize this approach on a series of tissue samples and to chronicle the underlying changes that occur from onset of malignancy and throughout disease progression.

1625 Fractal Dimensions and Lacunarity of Nuclear Distribution Separate Benign Tissue and Cancer Grades in Radical Prostatectomies

C Cheng, Z Ma, S Bhele, S Mohanty, Y-T Chu, D Luthringer, M Amin, B Knudsen, A Gertych. Cedars-Sinai Medical Center, Los Angeles, CA; University of Southern California, Los Angeles, CA.

Background: Lacunarity (L) and fractal dimensions (FD) are quantitative measures to assess the complexity of an image by measuring the geometric arrangement of its features. They describe repetitive patterns and structural heterogeneity of objects filling the image space. Since the arrangement of nuclei differs between benign and malignant glands, we hypothesize that by using FD and L to capture the topology of nuclei we will be able to distinguish benign glands, Gleason grade 3 (G3) and G4 cancer.

Design: High-resolution images were collected with the Leica scanner from 12 cases of radical prostatectomy and areas of equal size containing primarily benign epithelium (BE, n=25), cancer G3 (n=37), G4 (n=29) or stroma (ST, n=24) were identified by two pathologists. Hematoxylin images were deconvolved from H&E-stained images to generate a nuclear map using our previously developed algorithm. For analysis, binary nuclear masks and the hematoxylin images were uploaded into the FracLac plugin installed on ImageJ platform. A “gliding box” method was used to calculate FD and L in images of nuclear masks (FD(n), L(n)) and in Hematoxylin images (FD(h), L(h)) in areas of BE, G3 and G4. ST images were used as a reference. Results were evaluated with the Tukey’s Studentized Range test ($\alpha=0.05$).

Results: Analysis of nuclear masks and hematoxylin images provided different results. Measurements of FD(n) and L(h) were statistically different between areas of G3 and G4, G3 and BE and G4 and BE, but did not reach statistical significance in FD(h) and L(n). All four measures were significantly different comparing cancer and BE to ST.

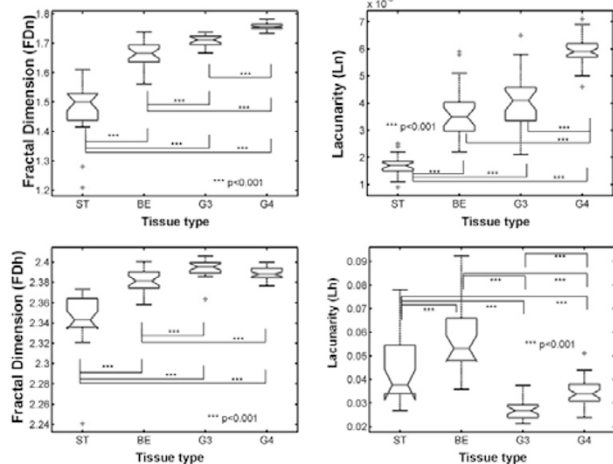


Figure 1. Fractal dimension and lacunarity distributions in tissue images (n- nuclear masks, h-hematoxylin images) from radical prostatectomies.

Conclusions: FD and L are complementary in their ability to discriminate architectural features of G3 and G4 from BE and G3 from G4. L is superior in measuring spatial heterogeneity and useful to differentiate between images with similar FDs. In future studies L and FD will be combined for a robust assessment of G3 versus G4 cancer, or percentages of area in categories of interest.

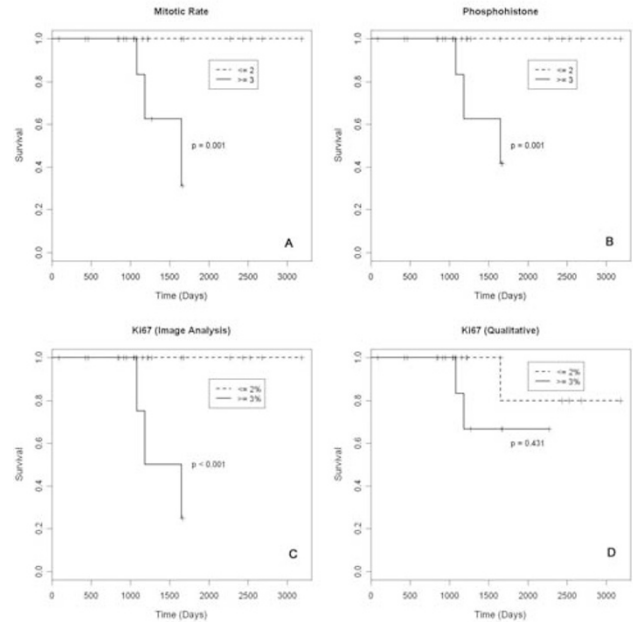
1626 Ki67 by Image Analysis and Phosphohistone H3 Are Objective Methods in Grading Pancreatic Neuroendocrine Tumors

A Cimic, AE Johnsen, W Harrison, JS Sirintrapun, RT Mott. Wake Forest Baptist Health, Winston Salem, NC; Memorial Sloan Kettering, New York, NY.

Background: Pancreatic neuroendocrine tumors (PanNET) account for 4% of pancreatic tumors. Most PanNETs are well-differentiated and have a low proliferation rate (<20 mitoses/10HPF). Predicting the clinical behavior of well-differentiated PanNETs remains controversial. PanNETs are graded as grade 1 (G1) based on mitotic count (<2) and Ki67 labeling index (<3%), or as grade 2 (G2) (> 2 and 3%, respectively).

Design: This study includes a series of 28 well-differentiated PanNETs with a median follow-up of 1265 days. The patients were predominantly female (N=18) and the median age was 54.7 years. Tissue microarrays (TMAs) were prepared in triplicate to include the most mitotically active areas. Immunohistochemical staining for Ki67 and phosphohistone H3 (PhH3) was performed. The Ki67 labeling index was measured using two methods, including an “eye-ball” estimate and image analysis using free software available online (Immunoratio.com). PhH3 was evaluated as the number of positive cells in 10 HPF. Results were correlated with clinical outcome.

Results: Four (14%) of the 28 patients had an unfavorable clinical outcome. Survival curves for mitotic rate, Ki67 (by image analysis), and PhH3 demonstrated a significant correlation with clinical outcome ($p<0.001$).



The “eye ball” method for determining the Ki67 labeling index was not significant ($p=0.431$) and often resulted in over-grading of the tumors.

Conclusions: Our results show that mitotic rate, Ki67 labeling index by image analysis, and PhH3 counts are all statistically significant at predicting survival. The traditional “eye ball” method of determining the Ki67 labeling index was not a significant predictor, emphasizing the importance of image analysis as a more reproducible methodology. The use of freely available online image analysis software should help to reduce interobserver variability and subjective interpretation of proliferative markers in the evaluation of PanNETs.

1627 HPASubC: Tools for High Throughput Subcellular Classification of Human Protein Atlas Images

TC Cornish, A Kapoor, A Chakravarti, MK Halushka. Johns Hopkins University SOM, Baltimore, MD.

Background: The Human Protein Atlas (HPA) is a comprehensive resource for immunohistochemical staining data for >18,000 antibodies targeting proteins from >15,000 genes. Staining has been performed on 42 normal tissues and 20 unique malignancies over numerous tissue microarrays (TMAs). Thus millions of individual cores have been stained and are available as images. HPA has characterized staining across these tissues into broad categories. However, for specialized staining patterns, such as intercalated disc (ICD) staining of the heart, no data is available.

Design: We created HPASubC to rapidly review and annotate images from HPA. The software is implemented as Python 2.7 scripts that use the standard library, BeautifulSoup4, and PyGame. From a list of ENSG IDs obtained at HPA, the scripts will download all relevant images. A PlayStation-style game controller is then used to rapidly review the images and tag those with the pattern of interest. An additional script can be used to assign a score of the user’s choosing (intensity, specificity, etc). Further scripts are designed to retrieve additional metadata for each gene/protein from the HPA site.

Results: We reviewed 49,200 cardiac images to search for ICD staining patterns. Across 3,000 reviewed images, the time spent per image averaged 0.57 seconds extrapolating to ~24 hours to review the entire set. We identified 1,691 images from 761 proteins that had ICD staining (~5% of HPA proteins). Of these 761 images, 300 (39%) had ICD staining on all cores available for review. Another 148 proteins (19%) had ICD staining in only 1 of 2 different antibodies suggesting heterogeneity in antibody quality. 176 proteins were identified by only a single positive core also indicating other sources of heterogeneity. All known ICD proteins, identified from prior studies, were confirmed using our method. The HPASubC tool has also been used to quantify non-myocyte staining patterns in heart tissue (endothelial cell, smooth muscle cell, etc) and additional subcellular patterns in the myocyte.

Conclusions: HPASubC is a new software suite to rapidly scan thousands of images and identify unique subcellular or subtissue staining patterns in HPA. It will allow a trained pathologist to find unique patterns within an enormous dataset of images. We have used it to significantly expand the number of proteins potentially found at the ICD.

1628 Just-In-Time Video Conferencing for Pathologists

DJ Cowden, ME Leon. H. Lee Moffitt Cancer Center and Research Institute, Tampa, FL.

Background: Just-in-time (JIT) web conferencing is a novel method that can be applied for video conferencing in which a pathologist captures a histological image from one microscope-mounted camera and, in real-time, projects it onto a remote multimedia device’s display (i.e. desktop computer, tablet, smart phone, etc). Using observational data, we have defined a model of satisfaction to assess the utility of JIT web conferencing.

Design: Six JIT web conferencing video streaming technologies (Join.me, gotoMeeting, TeamViewer, Yuuguu, WebEx, and SplashTop) are tested and observational data is recorded using questionnaires generated for both the hosting pathologist and

their downstream client/audience member(s). By applying the well-recognized microeconomic principle of utility: $[TUx = \text{Sum}(MUx)]$ (where TU is Total Utility and MUx is Marginal Utility), a model is derived. The observational data and derived model identify several relationships between satisfaction and overall utility (total and marginal). Observational data include connection times (downloads and plug-ins), latency effects, assessed reliability, available bandwidth, quality of remote access and image resolution (streamed to remote client device displays). Competing bandwidth demands were assessed and isolated (i.e. standard telephony supplanted the encoded-VoIP to avoid bandwidth collisions).

Results: The initial data obtained indicate that the web conferencing technologies with the shortest downloads/installations times scored the highest in overall satisfaction among hosting pathologists. Almost no perceived value was placed on the ability of the remote client to have remote control access for Just-In-Time Video Conferencing. Finally, the data from the end-user clients indicate that satisfaction is greatest when associated with highest resolution of the video streamed image.

Conclusions: Our initial assessment of total and marginal utility provides an effective model to represent the satisfaction of participants using Just-In-Time Video Conferencing. Based on the initial levels of satisfaction, Just-In-Time Video Conferencing appears to be a useful method for communicating with audience members for pathologists who need useful remote conferencing capabilities on short notice.

1629 Impact of Monitor Display Configuration on Digital Pathology Diagnosis

IC Cucoranu, AV Parwani, C Mello-Thoms, SE Monaco, WE Khalbuss, J Duboy, I Ahmed, K Espig, A Xithona, L Pantanowitz. University of Pittsburgh Medical Center, Pittsburgh, PA; University of Sydney, Sydney, Australia; Barco Healthcare, Beaverton, OR.

Background: Selecting the right digital display (monitor) to view and interpret digital images for diagnostic pathology use is important. The current impact of various display parameters on digital pathology has not been well studied, and no standardization or recommendation exists. The aim of this study was to identify critical display parameters and evaluate their effect on digital pathology diagnosis.

Design: 100 pathology glass slides (surgical pathology, cytology, special stains) were digitized (Aperio Scanscope XT scanner). Digital slides were evaluated by 3 pathologists using 6 Barco displays with varying parameter configurations. Display parameters evaluated were monitor size (30 vs. 24 inches), resolution (6 vs. 2 megapixels/MP), calibration (native vs. custom designed to modify color distribution), and luminosity (high vs. low). Glass slides were subsequently evaluated by the same pathologists using conventional light microscopy. For each case encounter image quality, diagnosis, diagnostic confidence (graded 1-10) and specific morphologic features were recorded. The percent of morphologic features difficult to identify was calculated.

Results: The 24inch/2MP display performed significantly better than the 30inch/6MP display. Luminosity did not have a significant impact. Both display sizes performed significantly better with native calibration compared to the custom calibration protocol. Diagnostic morphologic features were most difficult to identify with displays using a custom calibration protocol (Table 1).

Conclusions: These data show that digital display parameters can impact the detection of morphologic features necessary to render a diagnosis. Parameters that had a disadvantageous effect were calibration and monitor size, with a smaller effect caused by luminance. The best performance was obtained when using a 24 inch monitor without custom calibration.

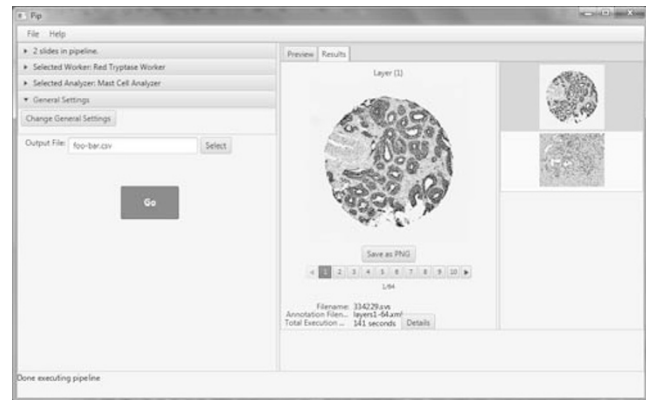
Table 1. Comparison of morphologic features with different monitor parameters.

Display Parameters				% Morphologic features difficult to identify
Screen size (inch)	Resolution (MP)	Calibration (custom/native)	Luminosity (high/low)	
30	6	custom	high	30.64
30	6	native	high	13.51
30	6	native	low	12.27
24	2	custom	high	24.5
24	2	native	high	8.29
24	2	native	low	7.71

1630 PIP: An Open Source Framework for Multithreaded Image Analysis of Whole Slide Images

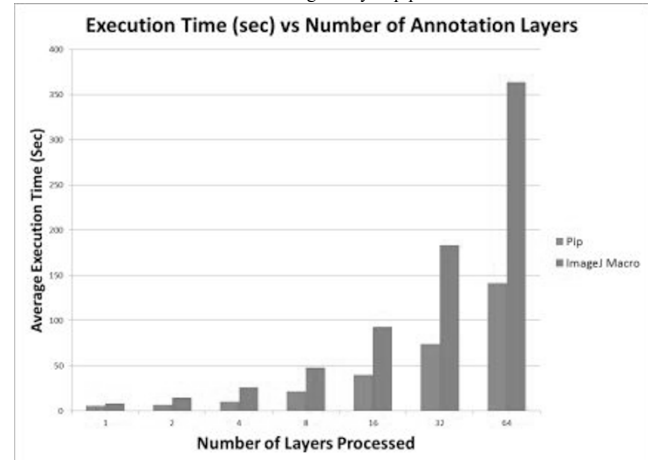
N Cuka, HA Hempel, KS Sfanos, AM De Marzo, TC Cornish. Johns Hopkins University School of Medicine, Baltimore, MD.

Background: Image analysis is a computational technique for extracting meaningful information from microscopy images. Whole slide images (WSI) are a convenient and increasingly popular substrate for image analysis in pathology. However, there are few open tools for image analysis on WSI using annotated regions of interest. To address this need, we developed PIP (PIP is for Image Processing), a Java-based software framework designed to apply arbitrary image analysis pipelines to WSI using a configurable thread execution model and inversion of control design principles.



Design: We evaluated the execution speed of PIP by comparing it to a standard ImageJ pipeline. A section from a tissue microarray (TMA) of prostate cancer cases was immunohistochemically stained for mast cell tryptase (Vector Red), cytokeratin 8 (DAB), and hematoxylin. The TMA was scanned as a WSI using an Aperio Scanscope, and 64 individual cores were manually segmented as annotation layers (0.64 mm² each) in Aperio Imagescope. A mast cell-counting algorithm was implemented as a macro in FIJI (FIJI Is Just ImageJ), and then translated to PIP using the ImageJ Java API. PIP directly read the WSI and annotation files. WSI segmentation for the macro was performed using a separate Java program prior to macro processing. Three trials were run using PIP and the macro for 1, 2, 4, 8, 16, 32, and 64 annotation layers per trial. Execution times were recorded and averaged.

Results: As the number of annotation layers increased, PIP significantly performed better than the macro for the tested image analysis pipeline.



Conclusions: We have demonstrated that the PIP framework provides several important features, including (1) native analysis of annotated WSI, (2) significant performance gains through intrinsic threading of operations, and (3) free and open source software implementation. Next steps for PIP include further performance tuning and ease of use enhancements.

1631 Using Peer-Reviewed Open Source Articles to Develop a Turkish Wordlist for Pathology Field

B Dursun, S Balci. TUBITAK, Ankara, Turkey; Yildirim Beyazit University, Ankara, Turkey.

Background: Wordlists and thesauruses for text mining studies in pathology field are not readily available for Turkish language. Open source data from peer-reviewed articles (such as abstracts in PubMed) are invaluable resources for text mining studies. Therefore, we developed a Turkish pathology wordlist from open source articles.

Design: Abstracts (from 2000 to 2004) and full texts (from 2005 to 2013) from Turkish Journal of Pathology website were imported to Oracle 11g database. A new word list was generated via tokenization. Tokens with 1, 2 and 3 character length and those containing numeric characters were excluded, because these were mostly abbreviations of diseases or protein names. Distinct tokens (words) from this list were compared to a Turkish open source Natural Language Processing library, Zemberek, which contains 1,140,208 words with alternative and complex forms (<https://code.google.com/p/zemberek/>). The words that are not common in each database were noted. Furthermore, the generated word list was also compared to MeSH list, in terms of exact match and string similarity (Oracle Jaro-Winkler string similarity method, >90% considered similar).

Results: 28820 distinct words were found in published articles. 16887 (58.6%) of them were common with Zemberek. 267 (0.9%) words were common with MeSH and 1870 (6.5%) were found to be similar to MeSH words. Others were mainly disease and tumor names, as well as procedural technical words, specific to pathology discipline. Of note, 185 words contained letters that are not included in Turkish alphabet also showing the usage of special names and terms from foreign languages.

Conclusions: 1) Published articles can be used to develop subject field specific word lists, thesauruses and dictionaries. These lists can be used for text mining researches, as well as pathology information systems. 2) The use of jargon is common among the Turkish pathology community, as expected to be true for any specific scientific group. Turkish pathology jargon contains nearly 40% different words from common wordlists and 6% similar words to MeSH list. This may be attributed to not only the interaction of pathology field with many medical disciplines, but also the use of international words in the common practice.

1632 Primary Diagnosis by Whole Slide Imaging (WSI) Telepathology: University Health Network (UHN) Goes Live

AJ Evans, B Perez-Ordenez, SL Asa. University Health Network, Toronto, ON, Canada. **Background:** UHN has been using WSI for diagnostic purposes, including frozen sections and consultations, since 2006. We recently completed a comprehensive 80 week WSI validation study in advance of using this technology to provide primary diagnostic services by telepathology to Lakeridge Health (LH), a large community hospital and regional cancer center located 40 miles east of Toronto. LH specimens are fully incorporated into our laboratory information system (LIS), allowing seamless reporting by pathologists located at either site. A WSI platform (Leica/Aperio ScanScope AT) was installed at LH to allow primary diagnosis by telepathology, a service intended to provide sub-specialty diagnoses while reducing turnaround time and largely eliminating the need to transport glass slides from LH to UHN.

Design: To ease our transition into primary digital reporting, we started with pathologists having the most experience using WSI for diagnostic purposes. All slides from the genitourinary, head & neck, endocrine and liver site groups are scanned initially at 20x. They are accessed through the LIS which is fully integrated with the WSI platform. While the intent is to report these cases by WSI alone, pathologists have the option of deferring a diagnosis to glass slide review and/or requesting slides be re-scanned at 40x.

Results: Between November 1, 2012 and September 30, 2013, 2354 cases (10569 slides; range = 1-74 slides/case) from the subspecialty areas noted above have been scanned and reviewed by 11 pathologists. Deferral to glass slides has occurred in 98 cases (4%). The most common reason for deferral has been pathologists seeking reassurance for a WSI diagnosis prior to sign out (81% of the 98 cases), followed by computer performance issues such as unacceptable pixelation (16%) and sub-optimal image quality in areas of diagnostic importance (3%). Only 1 case has required re-scanning of a slide at 40x. The WSI-LIS interface has broken down on 2 occasions, suspending our use of the system for 1-2 weeks with each occurrence while the problems were rectified. There have been no concerns over inaccurate or incomplete primary diagnoses made by WSI. **Conclusions:** UHN has successfully implemented WSI telepathology for primary diagnosis with 96% of cases reported without review of any glass slides. With increased computing power and our colleagues becoming more confident making diagnoses by WSI, we anticipate the deferral rate will decrease towards 1%. Episodes of WSI-LIS interface disruption have highlighted the importance of having backup access routes for LH digital slides.

1633 Quantitative Gaze Assessment of a Dual Whole Slide Image Viewer

SE Fox, C Law, BE Faulkner-Jones. Beth Israel Deaconess Medical Center, Boston, MA; Kitware Inc, Clifton Park, NY.

Background: Whole slide images (WSIs) are increasingly being used to train pathologists, however, the presentation methods most useful for diagnostic and teaching purposes are still being evaluated. Standard image presentation involves the examination of a single image at multiple levels of magnification. Placing two images "side-by-side" using a dual viewer yields new training capabilities. We present data on our use of a dual WSI viewer for diagnostic training, including remote eye-tracking visualization of gaze patterns among residents utilizing single and dual viewer functions.

Design: Trainees were recruited to compare and categorize WSIs from a large pre-existing teaching repository of classic dermatopathology cases, stored on our <https://slide-atlas.org> site and viewed using a dual image platform. The dual platform was displayed on a Tobii T-120 eyetracker over a client-server digital pathology system that supports fast web-based viewing over standard networks. Data, including gaze fixations and saccades collected by the eyetracker on a millisecond level, were used to quantify the visual exploration of images under different viewing modes.

Results: We present how the use of an advanced digital image software interface can assist in the diagnostic teaching process. Eye-tracking methods showed a reduced number of fixations within all tissue profiles during comparisons made with a dual image viewer as compared to exploration of the single WSIs. This corresponded to an overall increase in the efficiency of gaze pattern, similar to the pattern observed in experienced pathologists.

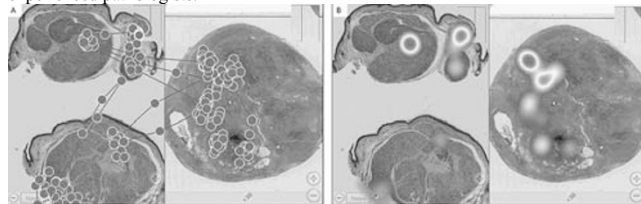


Figure 1: A) Resident fixation data and B) Heatmap of relative fixation time on WSIs within a dual image viewer.

Conclusions: Preliminary results demonstrate different patterns of trainee gaze during dual WSI comparison as compared to single image exploration. User interface features such as side-by-side viewing may increase the opportunity for targeting regions of fixation, and the training of efficient gaze patterns among residents.

1634 Primary Histopathological Diagnosis Using Whole Slide Imaging (WSI): A Validation Study

R Gerhard, A Honorio, A Gentili, MJ Brito, JM Lopes, FC Schmitt. IPATIMUP, Porto, Portugal; Faculty of Medicine, University of Toronto and University Health Network, Toronto, ON, Canada; Medical Faculty of Porto University, Porto, Portugal.

Background: WSI uses glass slides to obtain digital slides that reproduce conventional light microscopy original glass slides. WSI has been applied to different pathology fields, including teaching and education, research, quality assurance, and telepathology. However, it is still not quite validated as a primary tool for routine histopathological diagnosis. The aim of this study was to compare the histopathological diagnoses using WSI to routine light microscopy diagnoses from the original matched glass slides.

Design: Consecutive routine cases from biopsies and resections diagnosed during one month (April 2013) were studied. These cases were routinely diagnosed by a single pathologist using glass slides and light microscopy. WSI were obtained by scanning the original glass slides from all cases at 20x magnification, and evaluated by two different pathologists that were blinded to the routine histopathological diagnoses and clinical information. The digital and glass slides diagnoses were compared and classified as concordant, lightly discordant (without clinical implication), and discordant (with clinical implication).

Results: A total of 221 matched glass and digital slides from 189 biopsies and resections were analyzed. The digital and glass slides light microscopy diagnoses were concordant in 182 cases (96.3%). Seven (3.7%) discordances were found, including six lightly discordant cases. The only discordant case with clinical implication was from prostate biopsy where focal areas of adenocarcinoma were identified in two cores (routine glass slides), but misdiagnosed as benign using WSI. This case was reviewed and the diagnosis of adenocarcinoma was confirmed both on glass and digital slides.

Conclusions: The results of this study indicate that routine histopathological diagnosis based on digital slides is accurate when using the WSI technology. Indeed, the diagnoses concordance comparing digital to routine glass slides light microscopy, parallels reported concordance between pathologists when using the same glass slides for routine histopathological diagnoses.

1635 Diagnosis of Breast Needle Core Biopsies Using Whole Slide Imaging

S Goodman, D Kandil, A Khan. UMass Memorial Medical Center, Worcester, MA.

Background: Traditionally glass slides are examined and diagnoses rendered with the use of the microscope. With advances in imaging technology the possibility of utilizing whole slide scanning to render a diagnosis becomes plausible. The validation of digital pathology techniques is important for pathologists, clinicians, and patients to become comfortable with this new approach.

Design: 100 consecutive ultrasound guided breast needle core biopsies were reviewed from 2012 by author SG. One slide which best represented the original tissue diagnosis was chosen for use in the study. The slides were scanned at 20x magnification on a high resolution Ventana Whole Slide Scanner. Files were saved in the native JP2 format for viewing. Two pathologists (DK and AK), blinded to the original results, diagnosed the digital slides. Diagnoses were entered in a web-form which asked them to categorize each lesion into multiple categories such as benign, atypical, and malignant. In addition to further questions about the lesion, the form contained a questionnaire asking about slide quality and diagnostic confidence.

Results: The 100 scanned cases included: 22 malignant cases (1 lobular carcinoma, 1 solid papillary carcinoma, and 20 invasive ductal carcinomas (IDC)), 24 fibroadenomas, 8 fibroadenomatous changes, 3 intraductal papillomas, 1 atypical case, and 1 granular cell tumor. The remainder of cases was composed of a variety of benign breast tissues with fibrocystic changes. The first reviewer had a 99% (99/100) concordance rate with the original diagnoses. The second reviewer had a 98% (98/100) concordance rate with the original diagnoses. One digital case was called benign by 1 reviewer when the original diagnosis was suspicious for carcinoma. This case required additional workup originally and turned out to be invasive carcinoma on the resection specimen. The granular cell tumor was misclassified as IDC by 1 reviewer. The final discrepancy was a case called flat epithelial atypia (FEA) that was benign on the original diagnosis. FEA is known to have wide intraobserver variability, but can lead to different patient management. Diagnostic confidence was rated 10/10, extremely confident, on 88% of all cases reviewed, and the lowest confidence rating was 7/10 on 1 of 200 submissions.

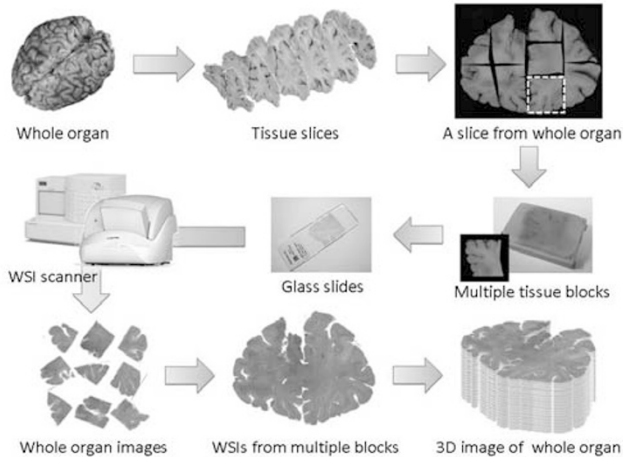
Conclusions: An average of 99% concordance between digital slides and the original diagnoses speaks to the strengths of digital pathology. This was accomplished without clinical history, immunohistochemistry, and multiple sections. The data speaks to the validity of whole slide scanning for a complete diagnostic workup and signout.

1636 Toward High-Resolution Whole Organ Histology 3D Model Development

N Hashimoto, J Taylor, T Tanaka, PA Bautista, M Snuderl, Y Yagi. MGH & Harvard Medical School, Boston, MA; Chiba University, Chiba, Japan; NYU Langone Medical Center and Medical School, New York, NY.

Background: The whole image of a tissue organ will allow us to observe the tissue at spatial perspectives not possible with a single histology slide. Being able to see the tissue at these perspectives could lead to the discovery of novel morphologic and growth patterns of human tumors. The high-resolution whole organ histology 3D model is advantageous to the discovery of the above mentioned patterns as it can improve the correlation between other modalities, such as MRI and 2D glass histology. However, the construction of this 3D model requires many steps, Figure 1. One whole organ can have 10s tissue slices wherein 1 slice can have 5-15 blocks, and from each tissue block 1000s of histology slides will be made. The average image and file sizes of a whole slide image (WSI) are 10 GB and 800MB, respectively; the estimated average

file size for the whole organ 3D model is 200TB. In this study, we have developed the technologies to: (1) piece together like jigsaw puzzle the images of the slides which belong to the same slice; (2) reconstruct the whole slice image from the (WSIs); and (3) view the reconstructed images in (2).



Design: We focused on a single slice of a whole brain tissue to develop the algorithms (1-3 in background). One slice of the whole organ was sectioned into 5-15 blocks. The H&E stained histology slides of the blocks were scanned with WSI scanners at 0.5um/pixel resolution. The WSI of a single slice is represented by the whole slide images of the blocks. The algorithms for whole slice image reconstruction and viewer were developed using the gross image of the organ and WSIs of the blocks.

Results: Automatic whole slice image reconstruction was developed and implemented by finding the appropriate position and rotation of the low-resolution WSIs through template matching. The reconstructed images can be comfortably viewed at , as if looking at one single large whole slide image, using the viewer we have developed.

Conclusions: We have developed the algorithm to reconstruct the high resolution whole slice image of a tissue organ and its corresponding viewer. This is an important step to reach our goal which is to create "high-resolution whole organ histology 3D model" in near future.

1637 Analytic Turnaround Time Study for Integrated Reporting of Pathology Results on Electronic Medical Records Using the Softek-Illuminate System

D Jacobus, T Karnik, Y Li, O Tawfik. Kansas University Medical Center, Kansas City, KS.

Background: Timely pathology results are critical for appropriate diagnosis and management of patients. Yet workflows in laboratories remain ad hoc and involve accessing multiple systems with no direct linkage between patient history and prior or pending pathology records for the case being analyzed. Because all clinical, radiological and laboratory data are essential to making correct diagnoses and appropriate management, this isolation of data causes unnecessary delay in the pathologists' workflows and can be detrimental to the quality and outcomes of patient care. These detrimental effects underscore the need for innovative workflow integration across multiple systems that facilitate the synthesis of data produced by the different specialties.

Our goal was to develop a comprehensive, user-friendly patient summary display to integrate the current siloed subspecialty-specific systems. We evaluated the Softek Illuminate PatientView application (Illuminate) for accomplishing this integration. Illuminate gathers information across hospital systems and provides instant access to patient history and all radiology, pathology and clinical laboratory results of prior procedures/visits to make better-informed decisions in real time.

Design: An analytical time study noting changes in TAT and pathologists' satisfaction with Illuminate were performed. The TAT before and after Illuminate implementation was recorded for 7 reviewers, including pathologists, residents and fellows. 15 to 20 cases of similar complexity were recorded per reviewer. Reviewers' TAT for 359 cases was recorded, including 200 cases prior and 159 post implementation. For each reviewer, time was recorded from the beginning of the case accession in the AP system (CoPath) until the time of signing out.

Results: Average TAT for all pathologists retrieving various information prior to Illuminate implementation was 5:32 min (range 10:50 to 1:35 min). That time was significantly reduced to 35 seconds (range 10 sec to 1:10 min). All reviewers were very pleased with the ease in accessing information and accepted eliminating the draft paper documents of the pathology reports, eliminating up to 65 min/day (25-65 min) by transcriptionists matching requisition with paperwork.

Conclusions: Utilizing Illuminate improved workflow, decreased TAT and minimized cost. Illuminate improves patient care through a comprehensive patient management system that facilitates communications between siloed clinical/radiology/laboratory systems.

1638 The Use of Machine Learning to Analyze the Features of Endometrial Malignant Mesodermal Mixed Tumors

A Kaplan, H-T Shiao, S Jackson, EL Dickson, AL Jonson, V Cherkassky, AM Truskinovsky. University of Minnesota, Minneapolis, MN.

Background: Malignant mesodermal mixed tumors (MMMTs) are clinically aggressive biphasic neoplasms of the female genital tract containing malignant epithelial and mesenchymal elements. We correlated histopathologic features of endometrial MMMTs with patient survival using machine learning, a novel, computer-assisted method, and compared the results with those obtained by conventional biostatistics.

Design: We reviewed the clinical histories and histopathologic material of the patients with endometrial MMMTs treated from 1952 to 2003. We recorded tumor size, depth of myometrial invasion, angiolymphatic invasion, cervical and serosal involvement, lymph node and other metastasis, the proportion of sarcomatous elements in the tumor, the presence of heterologous elements, proportion of squamous differentiation, mitotic count and the carcinoma type in each MMMT. Standard linear Support Vector Machine (SVM) with equal misclassification costs was used for the predictive modeling by machine learning. The linear SVM classifier is $f(w,x)=wx+b$, where x is the input vector and w is the weight for the features. The weights show which feature is more influential than others in the classifier. We also performed analysis of the influence of the histopathologic features on survival by using Kaplan-Meier curves utilizing the log-rank test for binary variables, Cox proportional hazards regression for all covariates and Wilcoxon non-parametric tests for continuous variables.

Results: We identified 37 patients, whose mean age at diagnosis was 66.6 years. Mean length of follow-up was 15 months. For those who died from disease, mean survival time was 13 months. By machine learning, other metastasis and the presence of undifferentiated carcinoma showed correlation with the output, death of disease ($w=1.933$ and 1.0 , respectively), while the proportion of squamous differentiation had a protective effect ($w=-0.2947$). Serosal involvement by the tumor significantly correlated with survival by Kaplan-Meier curves ($p=0.0004$) and the Cox proportional hazards model ($p=0.0112$). Non-parametric Wilcoxon two-sample test showed no influence on survival of the depth of myometrial invasion, mitotic count and the proportion of sarcomatous elements.

Conclusions: Machine learning can be used successfully to analyze histopathologic and clinical data and yields novel significant tumor characteristics. Analysis by machine learning suggests that the characteristics of the carcinoma underlying the MMMT correlate with survival.

1639 Use of Whole-Slide Imaging System for Frozen Section Diagnosis: Comparative Study between Virtual Slide and Glass Slide Interpretation

KK Khurana, A-LA Katzenstein, S Wojcik, LM Drogowski, N Drotar, O El-Zammar, S Landas, R Corona, V Baxi, M Montalo. SUNY Upstate Medical University, Syracuse, NY; Omnyx, LLC, Pittsburgh, PA.

Background: Advanced technology has made it possible to use whole-slide imaging to produce high quality analogs of microscopic tissue sections through digital scanning devices. The aim of this study was to assess the feasibility and accuracy of whole slide imaging for frozen section (FS) interpretation.

Design: Sequential FS along with touch preparation (TP), squash prep (SP) and smears slides at our institution were scanned using an Omnyx IDP 1.0 (VL4) digital slide scanner. FS whole slide images (WSI) and glass slides were independently reviewed by 4 pathologists who were masked to all prior results. The WSI scan time, the time taken to review whole slide images (WSI) for each pathologist, and image quality were recorded. The time required by the original frozen section pathologist to diagnose the glass slides (clinical read time) was also recorded. Correlation between the WSI and the glass slide interpretations was analyzed for each pathologist, and the quality of WSI and glass slides was compared.

Results: A total of 125 cases, consisting of 334 (304 FS and 17 TP, 10 SP and 3 smears) slides, were included. The average scan time per slide was 3.4 ± 2.0 minutes and per case 9.1 ± 6.0 minutes. Based on image quality there were only 6 slides (1.8%) in which a re-scan was needed for interpretation. The average time for pathologists reading the WSI was 2.1 minutes (range, 1.4-2.4) per case compared to the average clinical read time of 4.1 minutes per case. Concordance on categorical interpretation between WSI review and glass slide read for each pathologist was 100%. The image quality of WSI was comparable to that of microscopic glass slides in all cases.

Conclusions: The use of WSI for FS diagnosis compares favorably to conventional glass slide interpretation. The modest increase in FS turnaround time due to scan time may be partially offset by reduced review time needed by pathologists.

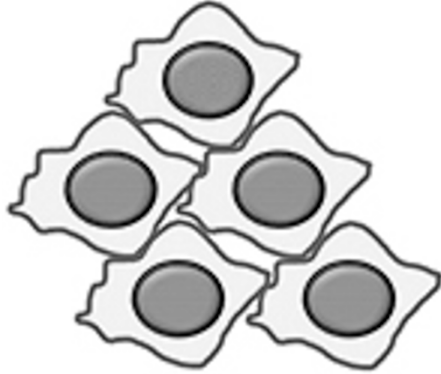
1640 Getting the Math Right: Development of a Robust Correction Algorithm When Using the Aperio Color Deconvolution Method for Quantifying Cytoplasmic Protein Expression

S-B Liang, MHA Roehrl. University Health Network, University of Toronto, Toronto, ON, Canada.

Background: Color Deconvolution (CD) is a commonly used computational tool in the Aperio software suite for the digital analysis of cytoplasmic signals. However, CD is only applicable to certain stains, because it does not differentiate cytoplasm from nucleus in cells. This characteristic often leads to large systematic errors when quantifying cytoplasmic protein expression. A correction of raw CD data is thus necessary to measure the expression of a marker more accurately.

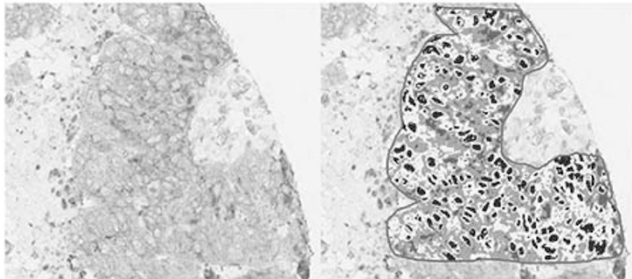
Design: To better reflect the real positivity status of cells, a series of mathematical formulas is developed that eliminate the contribution of signal from nuclear areas. The original CD and the corrected CD are evaluated for 4 cytoplasmic IHC markers on a total of 14,888 TMA cores from colon cancers.

Results: To illustrate the problem, when assuming a 1:1 area ratio of cytoplasm/nucleus, a group of cells with 100% 1+ positive cytoplasm (yellow) and negative nuclei (blue) is (incorrectly) scored by CD as 50% 1+ positive and 50% 0+ because the negative nuclear area is also counted (Figure 1).



	+	++	+++	-
Correct	100	0	0	0
CD	50	0	0	50

Two features of IHC signal distribution are useful. First, in weakly positive cells, positive signals are only located in cytoplasm. Second, as signal intensity increases, a portion of the positive IHC signal makes nuclear size appear seemingly smaller to the algorithm. A series of formulas is created to remove the influence of the nuclear contribution. These formulas were tested by correcting raw CD scores for the expression of cytoplasmic RON, FAK, pFAK, and SMAD4 protein markers in over 14 thousand tissue cores (Figure 2).



pFAK	+	++	+++	-
CD (uncorrected)	42.70	38.58	5.52	13.20
Correction (partial)	49.19	44.45	6.36	0.00
Correction (full)	26.50	64.30	9.20	0.00

Conclusions: Raw CD scores often result in systematically incorrect quantification of cytoplasmic markers. We show that these raw scores can be effectively corrected by a series of mathematical transformations that remove the nuclear influence of signals.

1641 Automated Annotation of Biorepository Samples with Digital Pathology Images

N Memon, S Costello, A Sharif. DSI, Cambridge, MA; Leica Biosystems, Dublin, Ireland.

Background: The recent advent and cost effectiveness of whole slide digital scanners allows tissue histopathology slides to be digitized and stored in digital image form. Thus far, this practice could not catch up with Biobanking because of its requirements for high network data-rate, large-volume storage and efficient thin-client architectures. Today, most of these technological deficiencies have been addressed except for the use of rich content, which can bring much to a biobank. Our team has integrated rich and plain content with an algorithm and technique that is automated, cohesive, light-weight, and scalable for Biobanks. This solution has made digital pathology a rich annotation for an integrated content approach for Biobanking in support of research and diagnostics for care providers.

Design: Adding rich content such as millions of pathology images, each with a substantial size, and keeping the response-time and storage requirements modest is critical for digital pathology. To accomplish this, we added another tier to the architecture. Rather than moving numerous bits around the network on every click, we show thumbnails of large images for each sample. It is only on specific requests from the users that we fetch the entire image and open a specialized web view with handy editing tools. Adding another tier to architecture introduces a problem of identity among related entities (Bank Samples and their Pathology Images in our case). We addressed this problem by using an identity hash-code between these entities. This solution works on SOAP protocol for web-based services. For performance enhancement, we have written proprietary user-authenticators and SOAP response parsers. We demonstrated this automated tool in our Biobanking application, Biomaterial Tracking and Management, (BTM™), with Leica-Aperio ePathology Suite and implemented it at UCLA.

Results: We were able to add rich media, and detailed digital imaging as annotations to

the banked tissue samples. With our solution, Digital Pathology can be an integrated, streamlined contribution to the research by enabling pathologists and biobankers to more efficiently illustrate, communicate, and collaborate on crucial findings in samples.

Conclusions: An integrated approach to data interpretation from banked samples is necessary for good research. With our solution, a richer media is added to Biobanking which can be used for visual inspection of tissue samples and web based consultations with expert pathologists for more efficient research in discovery, preclinical research and clinical trials design.

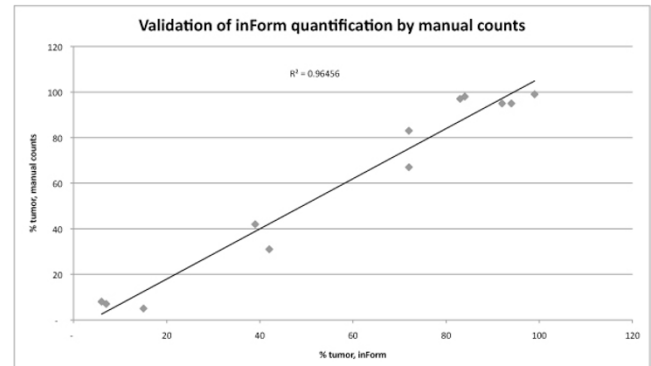
1642 Validation of Image Analysis Software to Quantify Neoplastic Cellularity in Tumor Specimens for Molecular Assays

MP Nasrallah, G Bocsi, CD Watt, RD Daber, MD Feldman. Hospital of the University of Pennsylvania, Philadelphia, PA; University of Colorado Denver, Denver, CO.

Background: Assessment of neoplastic cell content in a paraffin embedded tissue sample by a pathologist prior to molecular analysis is required to ensure the tumor burden exceeds the limit of detection for the molecular assay. In addition to significant interobserver variability in visually estimating tumor percentage, discrepancies between visual estimates and mutant allelic burden have been documented in clinical practice. We have investigated the use of a machine learning algorithm, inform®, Perkin Elmer Corporation, to improve estimation of tumor percentage.

Design: H&E-stained slides from four common types of cancer were scanned on an Aperio slide scanner at 20X magnification (n=12). A subset of the evaluated cases harbored *BRAF* V600E mutations (n=9). For these cases, *BRAF* mutant allelic burden was independently assessed by pyrosequencing and Next Generation Sequencing (NGS). Tumor and non-tumor nuclei in select fields of view from the digitalized slides were analyzed with inForm®, and the resulting neoplastic cell counts were compared with manual cell counts of the same fields to validate the software. inForm® was then used to analyze larger fields of the digital slides where macrodissection of the samples occurred for the *BRAF* mutant cases, and these inForm® estimates were compared with estimates derived from visual assessment by a pathologist and allelic burden obtained from pyrosequencing and NGS.

Results: Tumor percentages from manual cell counts correlated well with tumor frequency obtained using inForm®. Visual estimates tended to be lower than inForm® estimates. Tumor estimates from inForm® have a high degree of concordance with estimates from pyrosequencing and NGS, but the data suggest there are molecular mechanisms that can confound molecular estimates.



Conclusions: InForm® is a powerful tool for tumor percentage estimation, as these estimates are accurate when compared to manual counts and show visual estimates are frequently low. Use of the software becomes efficient as algorithms are refined with application to many tumors, but must be used with attention to the limitations of the current software.

1643 Whole-Slide Imaging in the Routine Diagnosis in Gynecological Pathology

J Ordi, P Castillo, M del Pino, O Ordi, L Rodriguez-Carunchio, R Millan, C Garcia, J Ramirez. Hospital Clinic-CRESIB, Barcelona, Spain.

Background: Whole slide imaging (WSI) is the process of digitizing glass slides, which enables the examination of pathology samples on a computer screen in a manner comparable to light microscopy. Although WSI has been used for different applications its use in routine diagnosis is still limited. This study aims to determine the accuracy of interpretation using WSI in the routine diagnosis of gynecological specimens as compared with conventional light microscopy (CLM), to understand the technology limits and possible interpretative pitfalls.

Design: All gynecological biopsies (small biopsies and surgical specimens) received at the department of pathology of the Hospital Clinic of Barcelona in July 2013, were analyzed blindly by two pathologists. One of them performed the diagnosis using CLM, which was considered the gold standard, and the second using WSI. For WSI, H&E slides were digitized in a Ventana iScan HT (Roche diagnostics) at 20x. The discrepancies were classified according to a modified Goldman classification as major (significant differences in clinical management or benign vs. malignant) or minor (no or minor clinical relevance). The results were evaluated by weighted Kappa statistics for two observations. Time spent by the technicians to charge the scanner and review the scanning process, and percentage of rescanning were also evaluated.

Results: A total of 351 cases, consisting of 966 glass slides, were evaluated; 48.4% of the biopsies were normal or had reactive lesions, 23.4% had benign tumors, 4.3% had low-grade premalignant lesions, 11.7% had high-grade premalignant lesions and 10.0% had malignant tumors. In 93.7% of the biopsies there was a complete agreement

between WSI and CLM interpretations. Major discrepancies were observed in 7 cases (2%); six of them consisted of underdiagnosed or missed small high grade squamous intraepithelial lesions of the cervix, and one was a lymph node micrometastasis of an ovarian carcinoma missed in the WSI evaluation. Minor discrepancies accounted for 4.3% of the biopsies. Interobserver agreement for WSI and CLM evaluations was at the almost perfect level (κ value: 0.904; 95%CI: 0.863-0.945). Mean time spent by the technician in charging and removing the slides from the scanner and verifying the adequacy of the scanning process was 25 seconds per slide. The percentage of slides requiring rescanning was 4.16% and the rate of scanning failure was 0.61%.

Conclusions: Diagnosis of gynecological specimens by WSI is accurate. Routine diagnosis and digital archiving of gynecological specimens by WSI may be introduced in departments of pathology.

1644 Iterative Segmentation Correction as a Substitute for Ground Truth

R Scott, J Zeineh, J Koll, FM Khan, C Cordon-Cardo, MJ Donovan, G Fernandez. Icahn School of Medicine, New York, NY.

Background: Evaluation and optimization of pathology-driven image segmentation algorithms is severely hindered by the difficulty of generating ground truth (GT) data. The current strategy to minimize GT bias, is for two or more pathologists to independently outline a given image into relevant histological regions. In practice, with current resource restrictions, it is often better to provide approximate GTs on a larger set of images. We have developed, tested and statistically justified a novel approach to GT entry that addresses these issues.

Design: Our GTA system allows the user to dynamically and interactively correct a prior segmented image thereby accepting or rejecting segmentation regions and classifications (eg. nucleus, cytoplasm, stroma) by clicking or touching regions via a specialized software interface on a high precision tablet. The user indicates whether a region is under or over segmented, and does not manually correct the outlines. Our guideline for GT entry is to correct ~90% of the algorithm's errors, which is sufficient for reliable algorithm evaluation, independent of the GT bias introduced by starting from a prior segmentation profile. The primary objective is to minimize user clicks. A secondary objective is to calculate segmentation accuracy metrics (sensitivity, specificity, Dice accuracy score) in real time, per image, to enable sorting, searching and visualization of image subsets. The size of the GT image set required depends on the variability of the images and the accuracy of the segmentation algorithm. The system calculates the image set size required for statistical significance depending on the current segmentation error rate. For smaller error rate the number of clicks required per image is reduced and the number of images is increased proportionately. A third objective is to support iterative evaluation and review of improved segmentation algorithms by reusing existing GT.

Results: The GTA was evaluated on a set of 266 prostate needle biopsy immunofluorescent images requiring 20 corrections per image on average, resulting in a Dice score of 0.89. GT entry time per image was approximately 4 minutes[M1] /image, or 17.7 hours in total for the entire image collection. To achieve statistical significance on the Dice score only 96 images were required with an associated decrease of 64%.

Conclusions: We have demonstrated a pathology-driven GT labeling tool based on correction of prior image segmentation that is an order of magnitude more efficient than prior outlining based systems. Rapid GT generation makes it practical to use large numbers of images for improving image analysis algorithms.

1645 The Use of Computer Vision for the Diagnosis of Benign and Malignant Smooth Muscle Neoplasms of the Uterus

M Shahi, X Li, A Kaplan, D Fehr, A Banerjee, V Morellas, N Papanikolopoulos, AM Truskinovsky. University of Minnesota, Minneapolis, MN.

Background: Following our successful application of computer vision to the diagnosis of epithelial neoplasms, carcinomas of the endometrium, prostate and breast, we use computer vision to diagnose benign and malignant mesenchymal tumors, leiomyomas and leiomyosarcomas of the myometrium.

Design: We analyzed digital images of hematoxylin and eosin-stained sections of 39 myometrial leiomyomas and 41 leiomyosarcomas, scanned at x50 magnification on a digital slide scanner. The leiomyomas were further subdivided into 32 usual leiomyomas and 7 leiomyoma variants, including cellular and epithelioid types. Each image was annotated using the annotation graphical user interface we developed earlier, sliced and stored in 150x150 image blocks. We obtained 10533 useful blocks from all classes. We applied k-nearest neighbor (k-NN) classification using region covariance features. We selected only texture features this time, i.e., I (intensity of the image), I_x , I_y (gradient of the image along x and y axis) and $\sqrt{I_x^2 + I_y^2}$ (its magnitude), ignoring the spatial information (x, y, ρ, θ) , allowing for a smaller feature space and accelerating the analysis, while still maintaining the quality. We performed a 10-fold cross-validation to test the performance of the k-NN classifier. One tenth of the samples was used as test samples, leaving the rest to build the database. We also applied tensor dictionary learning on region covariance features using the same setup as k-NN classifier, aided by Support Vector Machine (SVM), a new type of model-based classifier that searches for a hyperplane that best separates the two classes, fitted with the Radial Basis Function kernel to cooperate covariance features.

Results: The overall accuracy of distinguishing leiomyomas from leiomyosarcomas was 96.04% by the k-NN method and 94.45% by tensor dictionary learning on region covariance features with SVM support. Using the k-NN method, the accuracy of separating conventional leiomyomas from leiomyoma variants was 94.38%. Using the k-NN method, the accuracy of distinguishing usual leiomyomas and leiomyoma variants from leiomyosarcomas was 96.00% and 97.19%, respectively.

Conclusions: Our study shows that computer vision can be applied with high accuracy to the diagnosis of mesenchymal neoplasms, distinguishing myometrial leiomyomas from leiomyosarcomas and leiomyoma variants from usual leiomyomas. Human

pathologists are sometimes misled by the atypical features of the leiomyoma variants, but these features do not affect the ability of the computer to distinguish them from leiomyosarcomas.

1646 Applications of Google Glass [GLASS™ in Anatomical Pathology

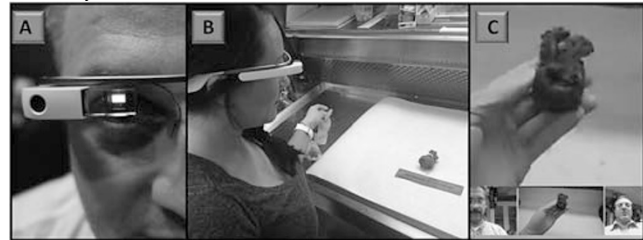
M Syed, I Ahmed, AV Parwani, C Saylor, J Nine, K Balatincz, J McHugh, BJ Kolowitz, J Taylor, G Michalopoulos, L Pantanowitz. University of Pittsburgh Medical Center, Pittsburgh, PA; University of Pittsburgh, Pittsburgh, PA.

Background: Google Glass (GLASS™) is a head-mounted, wearable computer that can connect to the Internet and display information in a smartphone-like, hands-free format. Glass has great potential in healthcare. Our aim was to explore the utilization of Google Glass in anatomical pathology.

Design: Glass (Explorer Edition) was operated with an extended external battery pack. A Google+ hangout account was established to share video and images. Glass was tested for use with gross telepathology and telemicroscopy. The Glass Mirror application programming interface (API) was evaluated to fine tune the pathologist interaction.

Results: Using Glass connected to the Internet during grossing permitted live video and audio feeds to be transmitted to all users connected to our Google+ hangout. Difficulties were related to optimal lighting, image resolution, frame freezing, taking snapshots during video calls, and hearing voice commands clearly in a noisy gross room environment. Telemicroscopy was unsuccessful because the camera failed to align with the microscope's oculars. Glass Mirror API provided mechanisms to manage timecards, interact with menu items, subscribe to timeline notifications, and share contacts. Current capabilities did not enhance user experience.

Conclusions: We report the first application of Google Glass technology in anatomical pathology. Our testing demonstrates that this novel apparatus can be employed to facilitate gross telepathology. Problems experienced with clinical implementation include network security and image quality. Further testing is in progress for additional pathology applications (e.g. autopsy service). Glassware customization with the Glass Development Kit (GDK) is planned when it becomes available to the development community.



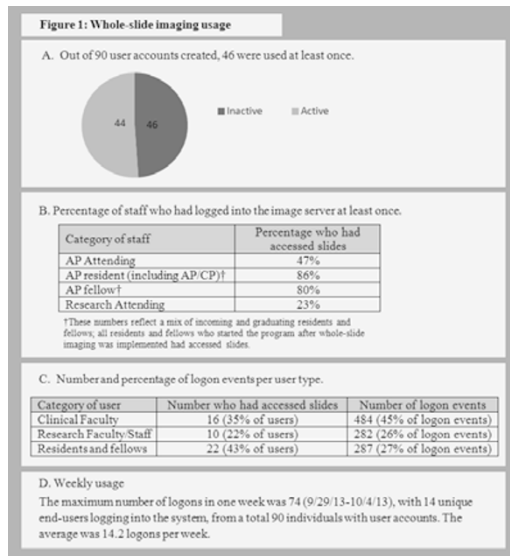
1647 Whole Slide Imaging Access and Retrieval

HC Tsang, CS Friedman, L Rivera, K Turner, V Brodsky. Weill Cornell Medical College, New York, NY.

Background: Whole-slide scanning is becoming increasingly prevalent, and numerous institutions have amassed significant databases of scanned slides. However, there is a paucity of data on how these slides are subsequently accessed and which types of scanned slides are the most likely to be accessed. In this study, we aimed to evaluate real-world data for whole slide imaging access and retrieval.

Design: During a 14-month period, slides selected by pathologists at our institution were scanned using the Aperio Scanscope AT (2012); Console version 101.0.4.413. The slides comprised a mix of clinical consult cases, educational slides, and research slides including tumor micro-arrays (TMAs). End users accessed the digital slides during this period via the web-based Aperio user interface (eSlide Manager). The image server access logs for the same time period were audited. Users were interviewed regarding their reasons for viewing the images.

Results: There were 1053 total unique logon events by 46 users accessing scanned slides. Of these, 178 logon events (17%) were to access clinical consult cases, 321 logon events (30%) were for educational slides, and 554 logon events (53%) were for research/TMA slides. In comparison, the percentage of scanned slides stored on the server comprised 76% clinical consult, 15% educational, and 9% research. The usage patterns are further described in Figure 1. Of note, the usage pattern included 7 individuals who jointly accounted for 64% of the logons. The three top reasons for viewing images, given by this group, were as follows: 1) to access research slides, 2) to access TMA slides and 3) to create lessons based on educational slides.



Conclusions: Research slides were accessed at a higher rate than other categories. Thus, research may represent the most high-yield category for the utilization of whole-slide imaging. Our analysis also suggested that a small number of pathologists who embrace whole-slide imaging can generate a high rate of usage of the system. A source of bias in our study may be low rates of access in the first several months of operation. Other sources of bias may be the continuous optimization of user permissions and slide grouping, as well as the changes in the types of slides scanned over time. A longer-term study of usage patterns is ongoing.

1648 Validation of Telepathology as a Consultation Tool between an Offsite Surgical Pathology Office Suite and Affiliated Tertiary Hospitals in the Frozen Section Diagnosis of Lung Neoplasms

T Vitkovski, T Bhuiya, M Esposito. North Shore LIJ Health System, Lake Success, NY.
Background: Frozen section on lung nodules can be particularly challenging. Inflammatory lesions can be difficult to differentiate from neoplasms. This is particularly challenging for junior and non thoracic pathologists who may require assistance from an expert thoracic pathologist. Increasingly, as in our institution, the operating rooms are located in tertiary hospitals and the pathology suite is located at a distant location because of offsite consolidation of pathology services. We aim to evaluate the utility of telepathology as a means to assist the pathologist at the time of intraoperative consultation of lung nodules when an expert pathologist is not immediately available to look directly at the slide.

Design: Two thoracic pathologists and 13 generalist/subspecialty pathologists participated. When the frozen section pathologist received a lung specimen with clinical impression of a neoplasm, he or she consulted the thoracic pathologist by telepathology utilizing a Nikon Digital Sight camera and web-based Remote Meeting Technologies software with live video streaming directed by the frozen section pathologist. The frozen section pathologist rendered a preliminary diagnosis and the thoracic pathologist noted the quality of the image and recorded his diagnosis. We compared the final diagnosis to both the diagnoses rendered at the time of frozen section.

Results: In 40 cases, diagnoses ranged from chronic inflammation to primary and metastatic carcinomas, lymphoma, sarcoma, and carcinoid. In 4/40 cases the image was of lesser quality (darker). The thoracic pathologist made the correct diagnosis in 100% of cases. 36/40 (90%) cases had 100% concordance amongst the frozen and thoracic pathologist in comparison with the final diagnosis. The thoracic pathologist made the correct diagnosis compared to the frozen section pathologist in 4/40 (10%) cases as follows: 2 adenocarcinoma versus AIS, 1 Non-small cell versus carcinoid, and 1 pleomorphic carcinoma versus inflammatory.

Conclusions: In this study of 40 cases of suspected lung neoplasm, the thoracic pathologist made the correct diagnosis in 100% of cases, thus validating the use of telepathology as a consultative tool in the frozen section diagnosis of challenging lung nodules. In the 10% of cases correctly diagnosed by the thoracic pathologist but misdiagnosed by the frozen section pathologist, 3 (75%) of those patients would have had suboptimal surgical resection had the frozen section pathologist not consulted the thoracic pathologist.

1649 Use of Digitized Whole Slide Imaging for Focused Professional Practice Evaluation of a Newly Hired Faculty Member

T Vitkovski, S Taboada, C Fan, C Torres, Q Chen, M Nasim, S Al-Atassi, J Crawford, T Bhuiya, J Bandovic. Hofstra North Shore-LIJ School of Medicine, Lake Success, NY.
Background: Focused Professional Practice Evaluation (FPPE) of a newly hired physician is mandated by Joint Commission. In the absence of set rules and timeline, various pathology practices follow different methodology to achieve that goal. We sought to explore the utility of Aperio whole slide imaging (WSI) to perform a focused review of a recently fellowship-trained GI pathologist in our department.

Design: Two experienced GI fellowship-trained pathologists and three senior general pathologists who participate in routine GI sign-out formed the core faculty to validate 30 test cases with neoplastic and non-neoplastic pathology chosen by the Chief of GI

pathology service for this study. None of the faculty was familiar with the system until being trained with a separate set of cases in preparation for this project. 30 cases (with 41 slides) of routine (15 cases), challenging (13 cases) and difficult pathology (2 cases) from 13 biopsy and 17 resection specimens were scanned in Aperio ScanScope® XT system. The two difficult cases were used to test the limitation of the system. Clinical history was provided. Tasks included simple diagnosis, recommendation of ancillary testing, and pathologic tumor staging (pre and post treatment). Considering the unfamiliarity with WSI, the following thresholds of correct diagnosis were deemed acceptable: routine: 90%; challenging: 85%; and difficult: 80%.

Results: The following is the breakdown of cumulative results of core pathologists: routine: 100%; challenging: 90%; and difficult: 70%. They did not meet the acceptable threshold of 80% for the two difficult cases. These cases included a microscopic focus of residual adenocarcinoma of the colon status post chemotherapy and a 0.8 cm gastric NET in a background of atrophic changes. Such cases are difficult on the glass slide as well and may not be suitable for FPPE. The new faculty member correctly diagnosed 14/15 routine cases (93%), 11/13 challenging cases (85%) and 1/2 difficult cases (50%). Limitations cited by the pathologists included measuring the size of lesions, magnification only up to 40X, quality of slides, and speed in evaluation of scanned slides.

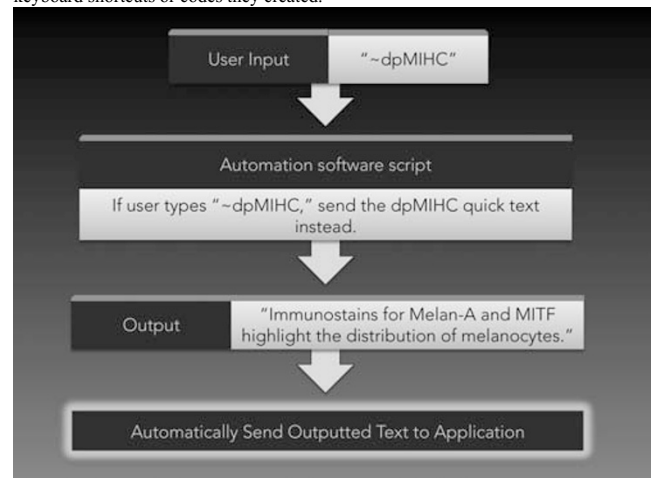
Conclusions: This study validated the use of WSI in a focused review of a fellowship-trained GI pathologist using routine and challenging cases. WSI is a fast and accurate method to achieve FPPE of a newly recruited pathologist in a short period of time. Rapid identification of knowledge gaps allows for the benefit of early initiation of further training and education.

1650 The Utility of Free Automation Software in Providing Universal Access to Pathology Templates/Quick Texts in any Program

JR Vu, J Ho, M Amin. UPMC, Pittsburgh, PA; Affiliated Pathologists Medical Group, Torrance, CA.

Background: The use of templates/quick texts (TQT) can improve the speed, efficiency and consistency of writing surgical pathology reports at lower costs than transcription-based services. While some pathology reporting software has built-in TQTs, generating and using custom TQTs can be problematic in institutions with multiple interfaces and software across different platforms. We evaluate the utility of a free and open source automation program, AutoHotkey (AHK) (Chris Mallet, autohotkey.com), in allowing pathologists to generate and use TQTs in any software program, system-wide.

Design: AHK was downloaded from the developer's website on all computers in our department. No administrator privileges were needed for installation. Once launched, AHK runs in the background of the operating system. TQTs are added and linked to keyboard shortcuts using an AHK script file, which is easily edited using any simple text-based editor (i.e. Notepad, TextEdit). Users insert TQTs into reports using the keyboard shortcuts or codes they created.



Results: AHK was used by both pathologists and residents in constructing reports. A total of 21,312 pathology reports over a 1-year period were constructed and signed out using TQTs created with AHK in applications such as CoPath Plus (v3.2, Cerner Corporation, Kansas City, MO) and Western Region System LIVE (v1.0, LabCorp, Burlington, NC). The mean turn-around-time per case decreased from 328 to 296 seconds; this amounts to 32 seconds of saved time per case, or 189.44 hours (7.89 days) of saved time in 1 year. Additional benefits cited by users included being able to use the same TQTs in any situation, including e-mails, presentations, pathology consultation websites and guides for training residents.

Conclusions: Free automation software utilities like AHK allow users to create, customize and share their own TQTs, regardless of software environment. It was integrated into our dermatopathology department's daily sign-out practices; it is also being used in smaller laboratories with anatomic/clinical pathology services. With no added cost, such utilities can provide an economical means of improving workflow in pathology practices.

1651 Accuracy, Precision, and Reproducibility Studies of the Philips Herceptest™ Using Manual Glass Slide and Whole Slide Image Review

DC Wilbur, E Brachtel, JR Gilbertson, J Vallone, S Krishnamurthy. Massachusetts General Hospital and Harvard Medical School, Boston, MA; University of Southern California, Los Angeles, CA; MD Anderson Cancer Center, Houston, TX.

Background: Scoring of HER2 immunohistochemistry (IHC) is currently performed using conventional microscopy on glass slides. The use of digital whole slide imaging has the potential to improve productivity, and allow remote interpretation and digital archiving of specimens. In order to implement such procedures, pathologist performance on digital specimens must be known and proven to be equivalent or better than the current standard of glass slide microscopic review.

Design: Inter- and intrapathologist reproducibility and precision between glass slide and digital whole slide imaging (Philips UltraFast Scanner and Image Management System) interpretation for negative (0-1+) and positive (2-3+) IHC scoring of HER2 in breast cancer were determined in 5 separate studies using Dako HercepTest-stained breast cancer slides. In 2 intermethod studies, 3 pathologists interpreted specimens; in the first study by glass and then by digital (180 cases), and in the second viewed in random order (184 cases). In both studies slides and digital images were reviewed in random order within the sets and there was a minimum of 7 days as a washout period between glass and digital interpretations. Two studies measured intra- and interobserver reproducibility and precision (1 pathologist each) and included 8 test slides (2 of each score) randomly intermixed with 12 non-test slides, read 10 times by both glass and digital methods (5 times each). Interpathologist reproducibility was determined by comparison to the reads already made in the first 2 studies above. One additional study evaluated the effect of adding IHC control slides with each run, using 1 pathologist interpreting 53 glass and digital slides randomized from the sets above along with appropriate controls for each slide in the set.

Results: The overall results of the intra- and interpathologist reproducibility and precision studies show that there is no statistical difference between the variance of performance when comparing glass and digital whole slide interpretations; and there were no positive or negative effects noted when control tissues were evaluated in conjunction with the test slides.

Conclusions: The results show that there is a similar outcome when interpreting HercepTest slides in breast cancer cases by either glass slides or digital whole slide images and this technology can be therefore be safely and effectively used for this purpose.

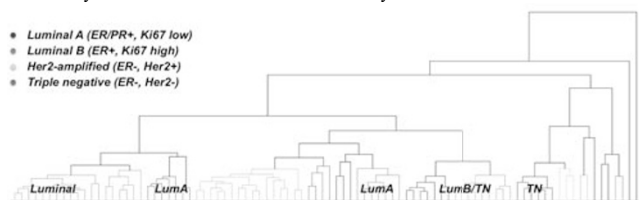
1652 Breast Cancer Subtype Classification from Computational Histological Image Analysis

MD Zarella, B Greenfield, J Yan, DE Breen, FU Garcia. Drexel University College of Medicine, Philadelphia, PA; Drexel University, Philadelphia, PA.

Background: Breast cancer is a heterogeneous disease encompassing multiple morphologies and different outcomes. Gene expression analysis has been used to classify breast cancer heterogeneity into at least four major subtypes, each with its own characteristics, sensitivity to treatment, and prognosis. Immunohistochemistry can be used as a surrogate for gene expression, yet both solutions are expensive and exhibit poor agreement.

Design: We developed a computational method that utilizes routinely available histological images to perform tumor subtype classification. This procedure uses image analysis to extract features that correspond to the nuclear properties and disruptions in normal organization that have been previously described. We then used a novel machine learning algorithm to transform the image features into a prediction of tumor subtype.

Results: We analyzed high-resolution whole-slide images of primary breast carcinoma specimens stained with a complete prognostic panel. Using cluster analysis, we discovered morphometric- and architectural-based subgroups that show moderate concordance with conventionally-defined subtypes from immunohistochemistry. Our analysis revealed a greater number of subgroups from morphometry than from immunohistochemistry, suggesting that additional subdivisions may exist that are not detected by traditional immunohistochemical analysis.



Next, we used a data set with a known ground truth to train a classifier based on nuclear morphology and show that 67% of cases are correctly classified using this method. Importantly, we show that this algorithm can be combined with immunohistochemistry to refine traditional subtype assignments, suggesting that there is information in both methods that can be exploited to improve categorization.

Conclusions: The successful development of a reliable algorithm to characterize tumor subtype based on histological image analysis can potentially be used to complement or even supplant existing tools. Consequently, it will expand the availability of this important diagnostic information to underserved populations.

1653 User Focused and Role Specific LIS and Digital Pathology System for Institutions Offering Multiple Molecular Assays

J Zeineh, R Scott, J Koll, F Khan, C Cordon-Cardo, M Donovan, G Fernandez. Mount Sinai, NY, NY.

Background: Use of multiple technologies at different points in the lab often stretches the limit of conventional LIS designs, especially when tests utilizing these new technologies (such as integrated image analysis and predictive modeling) involve workflows that didn't exist when the LIS's were designed. Inefficient solutions based on differing data models and communication methodologies are often implemented when legacy systems are made to work outside their original intent. To address these inefficiencies a new system architecture and reconceived user interfaces were created to support the high quality standards and growing needs of the pathology lab and its customers.

Design: A digital pathology workflow system was engineered with horizontally integrated infrastructure elements that synthesized data models and provided bilateral, rapid, reliable communications between components. Customized applications for different user roles were created that fused the required user specific functionality: pathologist, lab technician, customer support, and billing. To achieve test configurability, a mechanism was defined for modeling tests as separate state machines representing different workflows from accessioning to reporting.

Results: A lab-wide system was implemented to support specialized prostate cancer prognostics tests. Each test utilized a unique combination of H&E and multispectral fluorescent imaging with automated image analysis and predictive modeling. The system infrastructure components that supported the workflows included: Workflow Manager, Case Manager, Automatic Dispatching Service, Digital Image Manager, Analysis Server. A pathologist desktop application was created that fused all elements of the case (case data, workflow, image review, intralab communication, and reporting) and dynamically reconfigured itself based on the state of that case. Customized applications were developed for all other user types as well. For the prognostic prostate cancer tests, the mean time required for human interaction in generating test results with the new system went from 183.5 to 87.5 minutes. The average turnaround time for each test case decreased from six to three days.

Conclusions: This system proved to be significantly more efficient than the conventional LIS model interacting with adapted tools. Users reported greatly improved satisfaction in their interaction with the system and lab-wide communication. By providing a redesigned LIS with customizability at multiple points, advanced assay technologies are more easily translated from the research setting to viable laboratory performed tests.

1654 Block-Centric Visualization of Histological Whole Slide Images with Application to Revealing Growth-Patterns of Early Colorectal Adenomas and Aberrant Crypt Foci

N Zerbe, D Heim, J Kantonen, P Hufnagl, H Blaker. Charité - Universitätsmedizin Berlin, Berlin, Germany.

Background: Comfortable navigation and interaction are prospective challenges for acceptance of virtual microscopy applications in clinical pathology. Tracing suspicious and diagnostically important areas through multiple sections on one or more virtual slides is a typical task in slide reading. Currently this laborious and time consuming step has to be done manually by pathologists. Neither in conventional nor in virtual microscopy an alternation of multiple slides by retaining a relative position is currently feasible. We address this issue by presenting a method to read slides using computer assisted navigation more comfortable and intuitive. To demonstrate the methods strengths, we applied it to create visualizations of normal and adenomatous colorectal mucosal architecture by aligning hundreds of consecutive serial sections to reveal the different growth patterns.

Design: Histological images contain multiple distortions from different sources in the laboratory and digitalization process. We define several layers to provide a normalized representation of tissue. Each layer is associated with specific distortions and serves as a new level of abstraction. First layers enable a coarse alignment of tissue sections. Further alignment is achieved by multi-resolution feature point extraction and matching with subsequent geometric consensus filtering. Transformations from source to destination locations are calculated using corresponding pairs. Inside the convex hull of all fiducial points local affine transformations are applied whereas outside a global rigid transformation is used.

Results: The introduced method uses web services to deliver normalized image data as well as metadata. Additionally, a localization service provides a query interface to calculate corresponding image locations. Based on the introduced infrastructure, animated virtual stacks for regions of interest were reconstructed for growth-pattern analysis, disclosing new insights into the colorectal mucosal architecture.

Conclusions: Computer assisted navigation is an excellent tool to enhance clinical pathology. Beside an automatic alignment of serial slides pathologists are enabled to examine tissue sections of the same block independent of laboratory and scanner based distortions. Hence, slide reading shifts from a slide centric towards a block centric perspective.

1655 International Telepathology Consultation: An Experience from UPMC and Kingmed (China)

C Zhao, T Wu, X Ding. Magee-Womens Hospital of UPMC, Pittsburgh, PA; Kingmed Diagnostics, Guangzhou, Guangdong, China.

Background: Data about telepathology consultation service is very limited. Kingmed Diagnostics is a CAP certified large independent medical Lab in China. UPMC and Kingmed have established a telepathology consultation service for patients in China since 2012. The consultation is based on virtual microscopy digital files transmitted bilaterally between KingMed and UPMC Pathology.

Design: This is a retrospective study to summarize the telepathology consultation results from January 2012 to August 2013.

Results: The case numbers vary from 1-70/month with marked increase in the past 5 months with an average of 63 cases/month. The most cases is hematopathology, accounting for 23% of total cases, followed by bone/soft tissue pathology and gynecologic/breast pathology. Turnaround time varies depending on subspecialties. Average turnaround time was 6.8 days in 2012 and 4.9 days in 2013 ($p < 0.05$). Case distribution and turnaround time is listed in table 1. 59% cases submitted to the consultation were referred by pathologists, 38% by clinicians and 3% by patients. Malignant cases account for 67%, benign for 20%, and borderline/neoplasm for 13%. 88% of cases have a definite diagnosis, 8% with a favored/suggestive diagnosis, and 4% with an atypical/uncertain diagnosis. 226 (44%) cases were sent for consultation without primary diagnosis and 294 (56%) cases with a primary diagnosis or impression. Comparing diagnosis from UPMC with primary diagnosis in the 294 cases, the final diagnoses are the same in 21%, mildly modified in 24%, and significantly modified in 55%, which might affect treatment.

Categories	2012	TAT	2013 (Jan-Aug)	TAT
Bone/soft tissue	32	6.2	76	4.1
Breast/GYN	32	5.4	66	4.0
Head/Neck	17	7.7	28	5.8
Hematopath	2	6.5	119	5.9
GI	14	7.4	29	4.2
Liver	9	8.1	2	6.5
Thoracic	12	5.1	15	4.2
GU	11	11.4	14	6.4
Derm/Melanoma	7	3.9	18	6.0
Neuropath	5	6.0	5	3.2
Others	3	8.3	4	6.0
Total	144	6.8	376	4.9

Conclusions: Our results indicate that international telepathology consultation can improve patient care and safety through access to pathology expertise. The successful clinical service by international digital pathology depend on many factors, including strong commitment and support from leadership, IT experts, dedicated pathologists who understand language/culture on both sides. Many challenges still remain, such as internet speed, difference in cultures and health care systems, lack of clinical information, difficulties in communication with clinicians. Nevertheless, the international collaboration has had definite positive impact in patient diagnostic care through telepathology.

Kidney/Renal Pathology

1656 qRT-PCR Detection of BK Virus in Renal Biopsy Specimens from Renal Transplant Patients

RE Alexander, K Post, Z Zhao, K Meehan, C Phillips, L Cheng, J Lin. Indiana University School of Medicine, Indianapolis, IN; IU Health, Indianapolis, IN.

Background: BK virus infection in renal transplant patients is a constant concern due to the immunosuppressive therapies used in these patients. As BK-induced nephritis may lead to graft failure, detection of the virus in patients that allows for appropriate alterations in therapy is of significant clinical importance. While the diagnosis of BK virus infection can be made on H&E stained slides, the use of immunohistochemistry (IHC) has allowed for greater detection with higher specificity. The goal of this study was to compare the diagnostic effectiveness of using qRT-PCR to detect BK virus versus conventional light microscopic and IHC techniques.

Design: 65 renal biopsy specimens from renal transplant patients taken for evaluation of the presence for BK virus were selected. 26 of these cases had definitive histologic and/or IHC evidence of BK virus; the remaining 39 cases lacked sufficient evidence on either H&E or IHC. DNA extraction was performed on all cases and qRT-PCR was conducted. In addition, this process was also run on a "control group" of 49 renal biopsies taken from non-transplanted and non-immunosuppressed patients to establish specificity.

Results: In the 26 cases with definitive BK virus infection by H&E and/or IHC, qRT-PCR detected BK virus in 10 cases (62% sensitivity). In the control group of cases, no evidence of viral infection was shown by qRT-PCR with a specificity of 100%. Of the 39 cases with clinical suspicion of BK virus, but diagnosed as negative by H&E and/or IHC, qRT-PCR found 2 cases with BK virus. Analysis of these cases revealed that there was no viral inclusion on H&E, but no IHC had been performed. Subsequently, IHC was performed and showed focal BK positivity and confirmed the PCR detection.

Conclusions: These findings indicate that qRT-PCR is a highly specific detection method of BK virus, although the sensitivity is low when compared to traditional H&E and IHC methods. In light of these findings, the use of PCR may be particularly useful in cases with equivocal findings on H&E or IHC that can neither produce a definitive diagnosis or exclusion of virus. Despite its apparent lack of sensitivity, the high specificity of this modality infers its clinical utility in the proper context.

1657 Pulmonary Fibrosis-Renal Lipofuscinosis ("Black Kidney"), a New Disorder with Histologic Features of Hermansky-Pudlak Syndrome

N Aljinovic, AR Cullinane, BR Gochuico, WA Gahl, S Rosen. Beth Israel Deaconess Medical Center, Boston, MA; National Institutes of Health, Bethesda, MD; Harvard Medical School, Boston, MA.

Background: Membrane trafficking is an important cellular function and its failure is highlighted in Hermansky-Pudlak Syndrome (HPS), in which the functions of lysosome-like organelles are impaired by allelic mutations in one of 9 different genes. As a consequence, hypopigmentation is present in the skin, hair, and eyes due to defective maturation of melanosomes, and bleeding occurs due to the absence of platelet dense core granules. In addition, lipofuscin appears especially in the kidney, probably because

of defective lysosomal membrane turnover. HPS subtypes 1, 2, and 4 also manifest pulmonary fibrosis. The cause of this is unknown, but the type II pneumocytes have abnormally enlarged and abundant lamellar bodies. The characterization of 15 true mouse models of HPS helped identify murine and human HPS genes, largely through positional cloning. Kidney involvement is not overt in these mouse models, but renal lysosomal abnormalities have been documented both biochemically and by electron microscopy. Renal lipofuscinosis can be seen rarely in humans as an apparently solitary finding, but is common in some animal species, unassociated with kidney dysfunction.

Design: We present one family with pulmonary fibrosis and typical pneumocyte changes of HPS, renal lipofuscinosis and no platelet or oculocutaneous pigmentary abnormalities. The family had three brothers. Proband 1 and 2 died of pulmonary disease, and proband 3 has biopsy-confirmed pulmonary fibrosis. Proband 1 donated his kidney for transplantation; the kidney was refused because of its characteristic gross appearance.

Results: The lung biopsy in proband 3 showed peribronchial and septal fibrosis, hyperplasia and vacuolization of type II pneumocytes with extensive and giant lamellar body formation (electron microscopy). The explanted kidney of proband 1 showed abundant renal deposition of lipofuscin pigment and whole mount transmission electron microscopy revealed normal platelet dense granules. Genetic studies of proband 3 and two unaffected siblings showed that HPS related genes are not involved, but there is a unique mutation in a distinct gene containing a BEACH domain. Functional studies are underway to assess causality.

Conclusions: We present a new pulmonary-renal entity characterized by a fatal lung disease and marked renal lipofuscinosis, similar to HPS but with a distinct genetic mutation.

1658 Overload of Polyclonal Light Chains in Proximal Tubules Can Be Associated with Acute Tubular Injury and Interstitial Fibrosis

A Almradi, SC Wolforth, R Parasuraman, W Li, MT Rooney, PL Zhang. William Beaumont Hospital, Royal Oak, MI.

Background: Monoclonal light chains have been known to be nephrotoxic. Although serum levels of free polyclonal light chains (PLC) are found elevated in chronic kidney diseases by several groups, potential damage of PLC in the kidney has not been studied before. Our preliminary study showed that light chain staining by immunohistochemical method (IHC) was similar to that by immunofluorescent method in renal biopsies. This study was to determine whether overexpression of PLC in proximal tubules was associated with both acute renal injury and subsequent chronicity.

Design: Three groups of polyclonal cases included normal renal parenchyma from nephrectomy specimens ($n = 39$, normal controls), minimal renal disease ($n = 13$, MCD controls) and PLC study group composed of random native biopsies with various chronic kidney diseases ($n = 33$). They were all stained for kappa and lambda by IHC and their kappa staining scores (0 to 3+) were correlated with serum creatinine levels (sCr), periodic acid-schiff stain (PAS) scores for diminished brush borders (0 to 3+), and fibrosis scores on Trichrome stained sections (0 to 3+) using linear regression analysis.

Results: The two control groups had significant lower PAS and fibrosis scores when compared to PLC study group (by ANOVA). Taken 3 groups together, there were significant correlations between either sCr, PAS scores or fibrosis scores (on Y axis), and kappa scores (on X axis) as shown in the following table (* $p < 0.05 =$ significance).

Total n= 85	Kappa scores vs. sCr	Kappa scores vs. PAS scores	Kappa scores vs. Fibrosis scores
R value	0.42	0.54	0.66
Odds ratio	1.75	0.76	0.66
95% confidence interval	1.52 to 2.02	0.62 to 0.81	0.51 to 0.81
P value	0.0001*	0.0001*	0.0001*

Conclusions: Our data, showing significant association of PLC staining in the proximal tubules with acute and chronic renal injury, suggest that chronic overload of freely filtered PLC (due to their low molecular weights via glomerular filter barrier) in the proximal tubules can be nephrotoxic.

1659 Kikuchi Disease-Like Interstitial Necroinflammation in Renal Biopsies Associated with Autoimmune Disease: A Report of Three Cases

J Ambruzs, LN Cossey, R Lorschbach, CP Larsen. Nephropath, Little Rock, AR; University of Arkansas for Medical Sciences, Little Rock, AR.

Background: Kikuchi Disease (KD) is a rare, self-limiting disorder primarily involving lymph nodes and characterized by necrotizing histiocytic inflammation with prominent apoptotic debris. The etiology is unknown and few reports have shown an association with autoimmune disease but extranodal involvement has been described. We report the first cases of a KD-like necroinflammatory process occurring in the kidney in patients with autoimmune disease.

Design: We identified 3 native renal biopsies from our database with a primary finding of necrotizing lymphohistiocytic interstitial inflammation without evidence of infection or lymphoproliferative disorder.

Results: The cases involved two females and one male (14-40 years). Ethnicities included Native American, African American and Caucasian. All patients presented with fever, neutropenia, anemia, and elevated liver enzymes. One had documented lymphadenopathy. One patient had a history of mixed connective tissue disease while two had systemic lupus erythematosus. All cases had proteinuria, two had concurrent hematuria, and one had acute kidney injury. The most striking finding on renal biopsy was focal interstitial inflammation and necrosis characterized by amorphous eosinophilic debris and prominent apoptotic debris. All cases showed a predominantly T-cell lymphocytic and histiocytic infiltrate. A majority of T-cells were of the CD8+ cytotoxic type in two cases and scattered histiocytes showed MPO positivity. AFB and GMS stains were negative as was in-situ hybridization for EBV in all cases. There was mild, concurrent glomerular immune-complex deposition in two cases with no